



1 **Mapping Global Non-Floodplain Wetlands**

2

3 Charles R. Lane¹, Ellen D'Amico², Jay R. Christensen^{3,*}, Heather E. Golden^{3,*}, Qiusheng Wu⁴, and

4 Adnan Rajib⁵

5

6 ¹ U.S. Environmental Protection Agency, Office of Research and Development, Center for Environmental
7 Measurement and Modeling, Athens, Georgia, United States of America

8 ² Pegasus Corporation c/o U.S. Environmental Protection Agency, Office of Research and Development,
9 Cincinnati, Ohio, United States of America

10 ³ U.S. Environmental Protection Agency, Office of Research and Development, Center for Environmental
11 Measurement and Modeling, Cincinnati, Ohio, United States of America

12 ⁴ Department of Geography & Sustainability, University of Tennessee, Knoxville, Tennessee, United
13 States of America

14 ⁵ Hydrology and Hydroinformatics Innovation Lab, Department of Environmental Engineering, Texas
15 A&M University, Kingsville, Texas, United States of America

16

17 * These authors contributed equally to this work

18

19 **Correspondence:** Charles Lane (lane.charles@epa.gov) and Ellen D'Amico (damico.ellen@epa.gov)

20

21 **Abstract.** Non-floodplain wetlands – those located outside the floodplains – have emerged as integral
22 components to watershed resilience, contributing hydrologic and biogeochemical functions affecting
23 watershed-scale flooding extent, drought magnitude, and water-quality maintenance. However, the
24 absence of a global dataset of non-floodplain wetlands limits their necessary incorporation into water
25 quality and quantity management decisions and affects wetland-focused wildlife habitat conservation



26 outcomes. We addressed this critical need by developing a publicly available Global NFW (non-
27 floodplain wetland) dataset, comprised of a global river-floodplain map at 90 m resolution coupled with a
28 global ensemble wetland map incorporating multiple wetland-focused data layers. The floodplain,
29 wetland, and non-floodplain wetland spatial data developed here were successfully validated within 21
30 large and heterogenous basins across the conterminous United States. We identified nearly 33 million
31 potential non-floodplain wetlands with an estimated global extent of over 16 million km². Non-floodplain
32 wetland pixels comprised 53% of globally identified wetland pixels, meaning the majority of the globe's
33 wetlands likely occur external to river floodplains and coastal habitats. The identified Global NFWs were
34 typically small (median 0.039 km²), with a global median size ranging from 0.018-0.138 km². This novel
35 geospatial Global NFW dataset advances wetland conservation and resource-management goals while
36 providing a foundation for global non-floodplain wetland functional assessments, facilitating non-
37 floodplain wetland inclusion in hydrological, biogeochemical, and biological model development. The
38 data are freely available through the United States Environmental Protection Agency's Environmental
39 Dataset Gateway (https://gaftp.epa.gov/EPADDataCommons/ORD/Global_NonFloodplain_Wetlands/) and
40 through <https://doi.org/10.23719/1528331> (Lane et al., 2023).

41

42 **1 Introduction**

43

44 Wetlands are recognized as globally important ecosystems providing functions leading to critical
45 provisioning (e.g., food, fresh water for domestic, agricultural, and industrial use) and regulating services
46 (e.g., flood and drought mitigation, water purification and waste treatment, and habitat; Millennium
47 Ecosystem Assessment, 2005). Despite their functional importance, wetlands are threatened worldwide by
48 myriad anthropogenic disturbances, including sea-level rise (IPCC, 2014), drainage and filling (Davidson
49 et al., 2014), water abstraction (Liu et al., 2017), consolidation (McCauley et al., 2015), invasive species
50 (Zedler and Kercher, 2004), and changing precipitation and temperature patterns (Winter, 2000). These
51 widespread and globally prevalent alterations to wetlands affect their functioning, resulting in increased



52 downgradient flooding (Golden et al., 2021), modified stream baseflows (Buttle, 2018), reduced pollution
53 mitigation (Evenson et al., 2018a), and habitat loss (Uden et al., 2015).

54

55 Watershed-scale wetland management is currently hampered by the paucity of accurate and fine-grained
56 maps of wetland location (Creed et al., 2017; Christensen et al., 2022). However, methods to identify
57 existing aquatic systems, including wetlands, that provide functions at global scales have recently
58 emerged, such as the Landsat-based 30 m global surface-water inundation data (Pekel et al., 2016), finer-
59 resolution satellite-based landcover maps (e.g., Zanaga et al., 2021), and groundwater-driven aquatic
60 system characterizations (Fan et al., 2013). In addition, methods utilizing digital elevation models to
61 identify topographic depressions likely to support aquatic systems with characteristic wetland features,
62 such as saturated soils and/or ponded waters, have also regionally proliferated (Wu et al., 2019a; Wu et
63 al., 2019b; Christensen et al., 2022).

64

65 These advancements in mapping wetland location, such as those located within the river floodplain or
66 geographically distal from floodplains, allow resource managers to better incorporate wetland
67 biogeochemical, hydrological, and biological functions and concomitantly ecosystem services into their
68 decision-making efforts. For instance, incorporating *floodplain* wetlands into decision-making advances
69 the wise management and conservation of mapped riparian ecosystems (Tullos, 2018; Kundzewicz et al.,
70 2018). Thus, recognizing the importance of wetlands located within active river floodplains, land-
71 management decisions are being made to quantify the functions and ecosystem services of these wetlands
72 and incorporate them into watershed-scale hydro-ecological decisions (e.g., Makungu and Hughes, 2021;
73 Rajib et al., 2021).

74

75 However, *non-floodplain wetlands* are typically not incorporated into watershed-scale conservation and
76 management planning (e.g., Sullivan et al., 2019), thereby ignoring their contributions to watershed-scale
77 resilience in response to biogeochemical and hydrological disturbances (Rains et al., 2016; Golden et al.,



78 2021; Lane et al., 2022). Non-floodplain wetlands are abundant inland wetlands located distally from the
79 floodplains of rivers and lakes (Lane and D'Amico, 2016; Lane et al., 2018). Though typically small
80 (Cohen et al., 2016), high biogeochemical processing rates within non-floodplain wetlands have resulted
81 in these systems being termed bioreactors (Marton et al., 2015). Indeed, a literature review of over 600
82 articles found that the highest reactivity rates (pollutant mass removal per unit time) were found in the
83 smallest water bodies and wetlands (Cheng and Basu, 2017). Further, the high reactivity of individual
84 non-floodplain wetlands can cumulatively improve downgradient water quality conditions (Golden et al.,
85 2019; Evenson et al., 2021). Non-floodplain wetlands may therefore have an outsized impact on a
86 watershed's water quality.

87
88 Non-floodplain wetlands are also important ecosystems affecting water quantity (i.e., for storing and
89 gradually releasing water to downgradient rivers and streams). Specifically, precipitation is captured and
90 stored in non-floodplain wetlands prior to being discharged downgradient. During this storage period,
91 water can infiltrate to recharge aquifers, evaporate or transpire, or eventually “spill” overland and be
92 transported downstream (Jones et al., 2018; Buttle, 2018). These non-floodplain wetland water storage
93 functions attenuate storm flows (Shaw et al., 2012; Fossey and Rousseau, 2016; Blanchette et al., 2022)
94 and recharge groundwaters (Bam et al., 2020), thereby mitigating flood-hazards (McLaughlin et al., 2014)
95 and ameliorating drought conditions by maintaining baseflow (Ameli and Creed, 2019).

96
97 Despite the important functions provided by non-floodplain wetlands (Biggs et al., 2017; Chen et al.,
98 2022) a substantive data gap remains: no global maps or datasets exist identifying the geospatial location
99 of non-floodplain wetlands and open waters. Regionally focused efforts, such as the recent work by Lane
100 and D'Amico (2016) and Lane et al. (2022) mapped the extent of non-floodplain wetlands (also known as
101 geographically isolated wetlands, Leibowitz, 2015; Mushet et al., 2015) across the geospatially data-rich
102 conterminous United States (CONUS, see abbreviation list Appendix A). They found that 16-23 % of



103 freshwater systems were potential non-floodplain wetlands, suggesting a substantial yet hitherto unknown
104 portion of the globe's wetlands are likely also this vulnerable water resource.

105

106 Fortunately, geospatial data for identifying aquatic systems, including wetlands, are burgeoning (Khare et
107 al., in review). Global land cover and land use geospatial datasets that include a wetland cover class
108 continue to propagate (Hu et al., 2017a), taking advantage of both lengthy time-series Landsat data
109 (Homer et al., 2020) as well as recently launched advanced high-resolution and/or synthetic aperture radar
110 (SAR) equipped satellites (e.g., Sentinel-1, Sentinel-2, plus many commercially available platforms;
111 Martinis et al., 2022) and topographic data sources and analyses (e.g., Wu et al., 2019b). Examples
112 include the GlobeLand30 (Chen et al., 2015), the European Space Agency (ESA) WorldCover 2020
113 (ESA, 2020), the Dynamic World (Brown et al., 2022), as well as consortiums focusing on annual land
114 cover change mapping (e.g., Tsendbazar et al., 2021).

115

116 Lehner and Döll (2004) were amongst the first to publish a geospatially explicit global map focusing on
117 wetland extents. Their Global Lakes and Wetlands Database provides 1 km estimates of wetland
118 abundance. More recent and/or higher resolution wetland-focused datasets have emerged, including the 1
119 km global dataset from Hu et al. (2017b) that incorporates precipitation and a topographic wetness index,
120 and the multi-sourced 500 m composite maps of regularly flooded and groundwater-driven wetlands by
121 Tootchi et al. (2019). Tootchi et al.'s (2019) approach identified small and scattered wetlands. However,
122 they recognized the limitations inherent in their global product (ca. 500 m per pixel resolution) resulted in
123 omission errors for many wetland systems, especially those smaller than their 500 x 500 m (25 ha) data
124 resolution. This suggests, and Tootchi et al. (2019) acknowledged, that many (non-floodplain) wetlands
125 were omitted in the Tootchi et al. (2019) 500 m global product. Cohen et al. (2016) determined non-
126 floodplain wetlands in the CONUS are "unambiguously small", e.g., their average non-floodplain wetland
127 area was just over two hectares (2.1 ha). Based on the "all or nothing" methodological approach in
128 Tootchi et al. (2019), > 12.5 ha of a given 25.0 ha [one homogenous pixel] cell would have to be



129 identified as wetland in their resampling of the finer-scale data – much larger than the average 2.1 ha
130 wetlands found in Cohen et al. (2016).

131

132 Concurrent with increasingly available global land cover and wetland data, there is an increasing global
133 focus on deriving floodplain and flood-prone areal extents within river networks based on high-resolution
134 topographic data and hydraulic modeling (Tullos, 2018; Kundzewicz et al., 2018; Rajib et al., in review).
135 For instance, Sampson et al. (2015) created a global 90 m map of flood-prone areas between 60° N and
136 56° S. Nardi et al. (2019) developed a global floodplain dataset at 250 m resolution that extended from 60°
137 N to 60° S, based on geomorphic or terrain-based analyses of floodplain elevations. The evolution of the
138 MERIT Hydro 90 m global hydrography dataset by Yamazaki et al. (2019) has created additional
139 opportunities to further advance the derivation of global floodplains, with improved identification of flow
140 accumulation area, river-basin shape, and river channel location.

141

142 These wetland-location and floodplain-extent data are critical for watershed-scale sustainable aquatic
143 resource policy decisions (Creed et al., 2017; Golden et al., 2017). The lack of these data can result in
144 disproportionately large model errors and potentially misguided management decisions when non-
145 floodplain wetlands are not incorporated in hydrological and biogeochemical models, ignoring their
146 watershed-scale impacts on flooding, drought, and water quality (Evenson et al., 2018a; Rajib et al., 2020;
147 Golden et al., 2021).

148

149 Here, we provide the first global geospatial dataset of non-floodplain wetlands. We incorporate the recent
150 development of a high-resolution global floodplain mapping algorithm based on digital terrain models by
151 Nardi et al. (2019). We couple these spatial floodplain data with higher-resolution modifications to the
152 gridded global wetland and open water data layers developed by Tootchi et al. (2019) that incorporate the
153 Pekel et al. (2016) satellite-based inundation product, modeled groundwater-driven wetland extent (Fan et
154 al. (2013), and ancillary satellite landcover data from Herold et al. (2015). We test the applicability of our



155 global dataset of non-floodplain wetlands in 21 large and spatial-data rich watersheds across the CONUS.
156 This novel global product identifying non-floodplain wetlands provides for the quantification and
157 estimation of the locations and extent of important aquatic systems with abundant hydrological,
158 biogeochemical, and biological functions, filling a noted research gap while delivering useful data for
159 informed natural resource decision-making and management (Creed et al., 2017; Lane et al., 2022).

160

161 **2 Methodology and data**

162

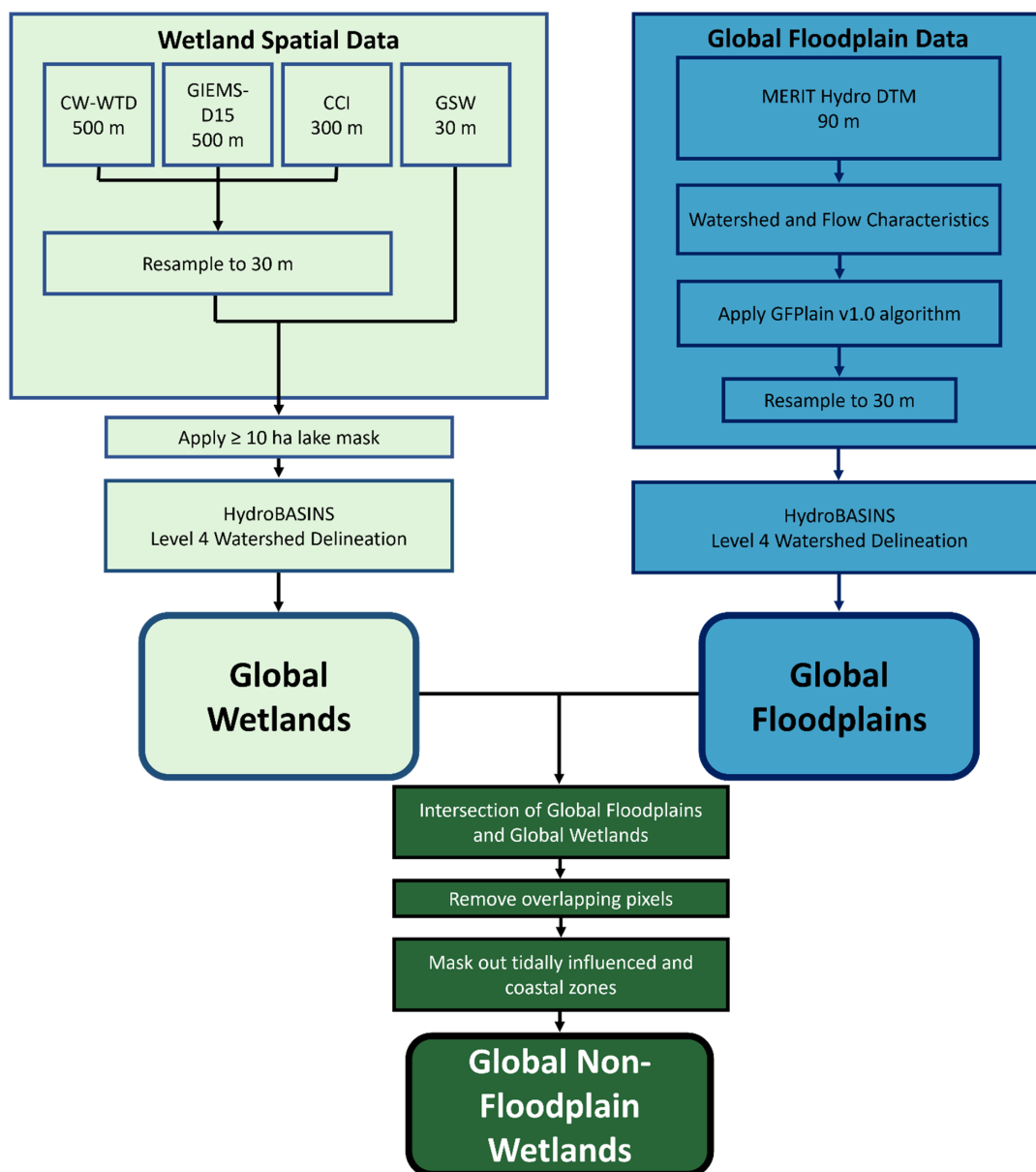
163 Identifying global non-floodplain wetlands required the following steps: 1) determination of global
164 floodplain extent, 2) identification of the global distribution of wetlands, 3) spatial overlay (masking) of
165 floodplains and wetlands to derive a non-floodplain wetland data layer, and 4) data verification and
166 accuracy assessment. Steps 1-3 are outlined in a flow chart given in Figure 1.

167

168 **2.1 Global floodplain data**

169

170 Nardi et al. (2019) combined space-borne elevation data and terrain analysis with a novel open-source
171 algorithm to delineate the geomorphic floodplains across the globe between 60° N and 60° S latitudes.
172 Conceptually, Nardi et al. (2019) identified floodplains from surrounding hillslopes as those low-lying
173 landscape features that have been naturally shaped by accumulated geomorphic effects of past flood
174 events. The original Nardi et al. (2019) dataset was limited in its spatial extent (60° N-60° S) and
175 resolution (250 m); this study sought to delineate global floodplain extent while concurrently identifying
176 floodplain features further up the river network than possible with 250 m pixels. Hence, we utilized the
177 freely available Nardi et al. (2019) GFPlain v1.0 algorithm and coupled this with the MERIT Hydro
178 (Multi-Error Removed Improved Terrain, Yamazaki et al., 2019), global raster digital terrain model data
179 to develop a higher resolution (90 m) geomorphic riverine floodplain for the globe, termed hereafter
180 GFPlain90.



181
182 **Figure 1.** Data flow chart identifying the main data sets and processes involved in deriving the Global Floodplain
183 and Global Wetland data layers, as well as the intersection of those data to create the Global Non-floodplain
184 Wetlands data product. Curved boxes represent final products, and abbreviations may be found in the text and
185 Appendix A.



186 The development of GFPlain90 required multiple steps. We first extracted elevation data from MERIT
187 Hydro, reprojected the data in UTM zones to prevent distortion when using the GFPlain algorithm, and
188 then developed the drainage network, drainage area, flow accumulation and flow direction data from
189 these data using the scaling parameters in Nardi et al. (2019). We established 20 km² as the minimum
190 contributing-area threshold required to create the drainage network, balancing the development of a
191 global stream-network distribution and extent with computational requirements. We then globally
192 organized the data by HydroBASINS Level 4 basins (Lehner and Grill, 2013). HydroBASINS provides
193 seamless watershed boundaries and subbasin delineations at global scales; there are 1,342 Level 4
194 HydroBASINS globally. The floodplain extent resolution of GFPlain90 was resampled (using nearest
195 neighbor) to 30 m for subsequent performance assessment and overlap analyses with the wetland spatial
196 data. All spatial analyses in this study were conducted using ArcGIS Pro v.2.9.x (ESRI, Redlands,
197 California) and GRASS GIS v 7.4.4 (OSGEO, Beaverton, Oregon).

198

199 **2.2 Global Wetland data**

200

201 Tootchi et al. (2019) developed a widely used composite global wetland map at ~500 m by combining
202 multiple data sources, including both satellite-based surface-water inundation mapping and vegetation
203 classification coupled with model-based approaches capturing important groundwater-driven wetland
204 systems. We specifically used the Tootchi et al. (2019) composite map consisting of both regularly
205 surface-water flooded and groundwater discharge-maintained wetlands as the foundation for our global
206 wetland map.

207

208 **2.2.1 Original composite wetland data**

209

210 Regularly flooded wetlands (RFWs) derived by Tootchi et al. (2019) were based on three data sources: 30
211 m resolution Global Surface Water (GSW) by Pekel et al. (2016), 300 m Climate Change Initiative (CCI)



212 land cover data by Herold et al. (2015), and 500 m GIEMS-D15 wetland extent data by Fluet-Chouinard
213 et al. (2015). GSW data used by Tootchi et al. (2019) were developed from Landsat satellite imagery
214 analyses of pixels identified as inundated at least once during the 32-year period of record by Pekel et al.
215 (2016). CCI input wetland data for Tootchi et al. (2019) included both inundated and wetland vegetation-
216 classed pixels assessed during the period 2008-2012 by Herold et al. (2015). For GIEMS-D15, data
217 included were the mean annual maximum extent of pixels identified as wetlands using multi-sensor
218 satellite data by Prigent et al. (2007), downscaled to ~500 m resolution by Fluet-Chouinard et al. (2015).
219 GSW and CCI input data were resampled to ~500 m resolution using an “all or nothing” approach by
220 Tootchi et al. (2019). This means that a pixel categorization of “wetland” at 500 m resolution was given
221 by Tootchi et al. (2019) only if the majority of resampled finer-resolution input pixels were classed as
222 wetlands. The resampling from 30 m and 300 m to 500 m resulted in a loss of informative spatial data on
223 wetland extent from GSW and CCI. Tootchi et al. (2019) calculated that RFWs cover approximately 9.7
224 % of the global land area (excluding lakes [sourced from (Messenger et al., 2016)], Antarctica, and the
225 Greenland ice sheet).
226
227 Groundwater-driven wetlands (GDWs in the analysis of Tootchi et al., 2019) used in this study were
228 based on the water-table depth estimates by Fan et al. (2013). Fan et al. (2013) developed a 1 km
229 resolution groundwater map based on climate and terrain variables that was validated by over 1 million
230 government-recorded and published observations. Fan et al. (2013) estimated that shallow groundwater
231 influenced nearly 15 % of groundwater-fed surface features, explaining important wetland patterning at
232 global scales (as well as vegetation classes at local and regional scales). A water-table depth threshold of
233 ≤ 20 cm was used by Tootchi et al. (2019) to identify groundwater-driven wetlands and they resampled
234 these data to ~500 m cell resolution. The GDW distribution based on water table depths covered
235 approximately 15 % of the global land mass (including large portions of the Amazon basin, coastal zones,
236 and North American and Siberian peatlands).



237

238 Tootchi et al. (2019) merged the RFW and GDW maps to form a union product with a high correlation
239 with available evaluation data, which they called the composite wetland-water table depth (hereafter CW-
240 WTD). They measured an approximately 3.8 % overlap between the total land pixels identified as
241 wetlands in both the RFW and GDW maps that comprise the CW-WTD, suggesting the different input
242 maps capture different wetland types. At the global scale, Tootchi et al. (2019) reported spatial Pearson
243 correlations between CW-WTD (wetland fractions at 3 arcmin, or ~4.9 km grids) and wetlands within
244 GLWD (Lehner and Döll, 2004) and Hu et al. (2017b) as $r=0.34$ and $r=0.43$, respectively. Tootchi et al.
245 (2019, their Table 5 and S1) provided additional analysis of the correlations between their global wetland
246 product and existing benchmark data. The total CW-WTD global wetland estimate was ~ 21.1 % of the
247 land mass, or approximately 27.5 million km^2 (excluding large lakes, Antarctica, and the Greenland ice
248 sheet; Tootchi et al., 2019).

249

250 **2.2.2 Derived global wetland data**

251

252 To account for the acknowledged limitations of the Tootchi et al. (2019) data and to accurately identify
253 more of the existing small and, specifically, non-floodplain wetlands across the globe (e.g., those <25 ha),
254 we improved upon and augmented the CW-WTD (Tootchi et al., 2019) global wetland data layer with the
255 30 m native-resolution GSW (Pekel et al., 2016) and 300 m native-resolution CCI (Herold et al., 2015)
256 data. The inclusive wetland categories of Tootchi et al. (2019) were maintained, namely at least one
257 inundation event over a 32 year range (for GSW data) and CCI pixels defined as “...mixed classes of
258 flooded areas with tree covers, shrubs, or herbaceous covers plus inland water bodies...” (Tootchi et al.,
259 2019, p. 193). However, for our analysis we resampled the 500 m CW-WTD product to 30 m using the
260 nearest-neighbor approach and then added any identified wetland pixel from the CCI data (resampled
261 from 300 m to 30 m) and inundated pixel from the GSW data (30 m resolution). Resampling to a finer
262 resolution does not result in a loss of any data whereas resampling from a finer resolution to a coarser



263 resolution results in the loss of any data smaller than the chosen resolution. This resulted in a novel and
264 encompassing wetland ensemble end-product, hereafter termed the Global Wetlands dataset. This new
265 dataset is inclusive of both finer-resolution (30 m) data, thereby accounting for a wide range of wetland
266 sizes – such as smaller non-floodplain wetlands (Cohen et al., 2016) – that remained unmapped by
267 Tootchi et al. (2019).

268

269 **2.3 Global Non-Floodplain Wetlands (Global NFWs)**

270

271 To identify non-floodplain wetlands specifically, we overlaid our GFPlain90 floodplain data with our
272 mapped Global Wetlands data to mask wetland pixels collocated on the floodplain. Then, to avoid tidally
273 influenced wetlands, we conducted a region-group analysis to identify connected pixels abutting coastal
274 shorelines in order to mask wetlands in coastal areas (e.g., those directly abutting the shoreline and
275 spatially connected to tidally influenced areas). We used a four-directional contagion criterion to identify
276 connected pixels (i.e., those connected in cardinal directions). Subsequently, we applied a 1 km buffer to
277 the HydroBASINS (Lehner and Grill, 2013) coastline area and removed from our analyses any wetland
278 region-group partially or completely overlain by the 1 km coastline buffer. In addition, Tootchi et al.
279 (2019) removed lake systems (≥ 10 ha) from their wetland-focused data by masking aquatic layers using
280 HydroLAKES (Messenger et al., 2016). To avoid including large lakes in our emerging non-floodplain
281 wetland geospatial data, we also applied the HydroLAKES mask and removed lake systems ≥ 10 ha
282 (Messenger et al., 2016) from our Global Wetlands dataset. Thus, our final global non-floodplain wetland
283 data product (hereafter Global NFWs) did not include fluvial floodplain wetlands nor coastal wetland
284 complexes and large open water lacustrine (lake-like, Cowardin et al., 1979) systems.

285

286 **2.4 Data verification and assessment**

287



288 We evaluated the global products developed here through comparison of high-resolution floodplain and
289 wetland extent data from 21 basins representing disparate climatic (according to the Köppen-Geiger
290 classification, Beck et al., 2018), elevation, and land-use gradients within the CONUS (Fig. 2;
291 summarized in Table B1). We specifically focused on the CONUS for product assessment because of its
292 wide-ranging data availability and diversity of physiographic and climatic regions.

293

294 **2.4.1 Verifying floodplain extent**

295

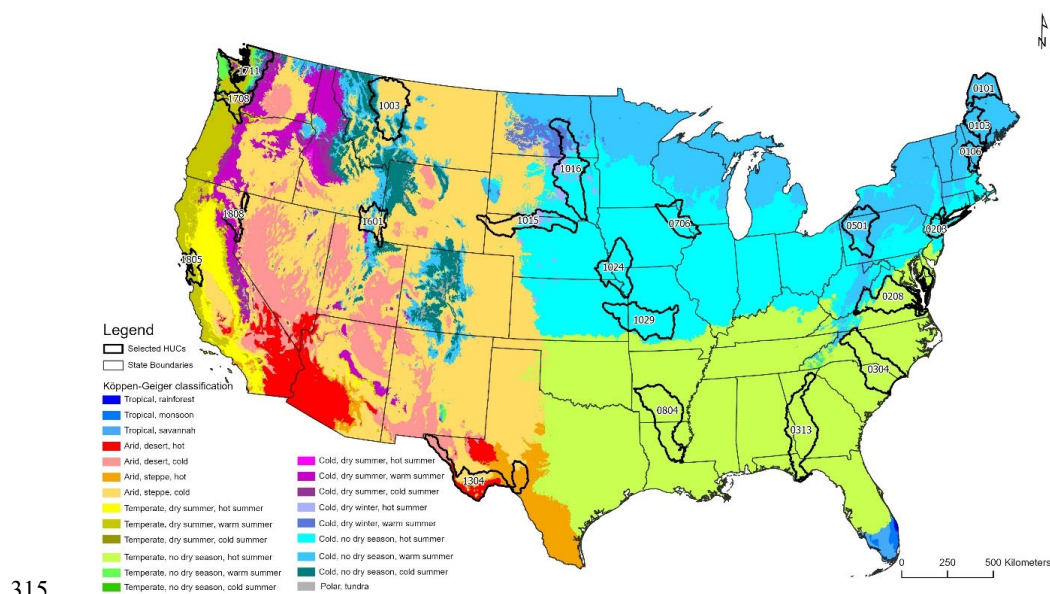
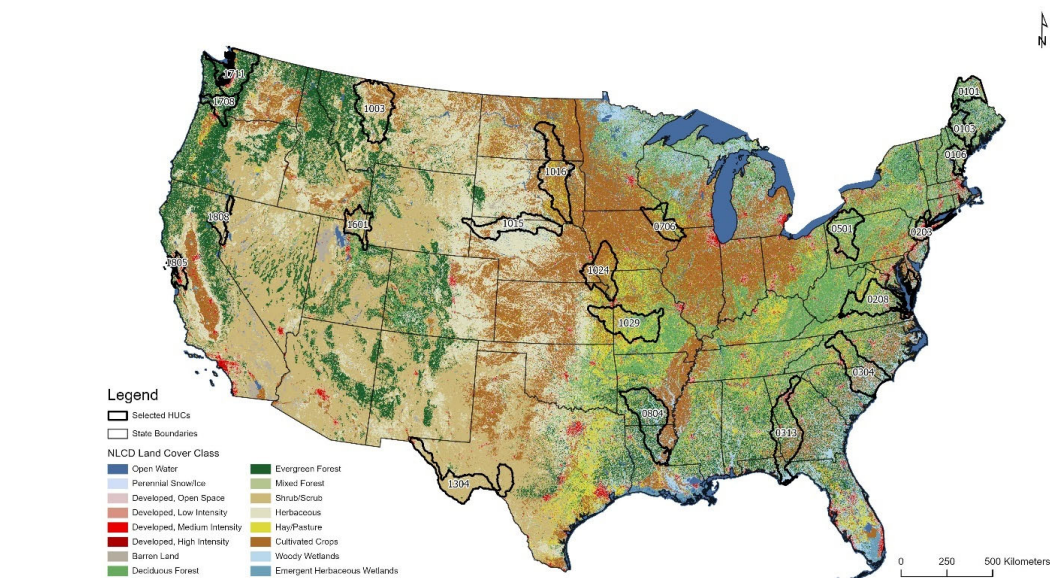
296 We used a recently developed machine learning (ML)-based 30 m resolution CONUS floodplain dataset
297 (Woznicki et al., 2019) as the benchmark to evaluate our GFPlain90 global floodplain data. Specifically,
298 the ML model by Woznicki et al. (2019) used the U.S. Federal Emergency Management Agency (FEMA)
299 100 yr floodplain (i.e., a 1 % chance of coastal or fluvial flood-inundation in a given year; Jakubínský et
300 al., 2021) as the training data, and subsequently used soil and topographic characteristic along with land
301 cover to identify potential floodplain grid cells across CONUS at 30 m resolution. Woznicki et al. (2019)
302 reported that their ML approach correctly identified ~79 % of the FEMA 100 yr coastal and fluvial
303 floodplains, providing spatially complete 100 yr floodplain coverage totaling 980,450 km² across the
304 CONUS.

305

306 **2.4.2 Verifying wetland and non-floodplain wetland extent**

307

308 We evaluated our inclusive Global Wetlands and Global NFWs datasets in 21 basins covering ~680,000
309 km² (Fig. 2). We contrasted our products to the 2016 National Land Cover Database (NLCD, Dewitz,
310 2019). The NLCD is a 30 m Landsat satellite-based geospatial product with an overall accuracy of 86 %
311 that incorporates high-resolution aerial imagery of wetland location for model parameterization and
312 calibration (Jin et al., 2019; Wickham et al., 2021). Three NLCD classes were selected for comparison
313 with the Global Wetland product: woody wetlands, emergent herbaceous wetlands, and open water. To



316 **Figure 2.** Twenty-one validation watersheds were selected from across CONUS to capture the breadth and extent of
 317 land use (top) and climate and physiographic regions (bottom) within CONUS according to the Köppen-Geiger
 318 classification (Beck et al., 2018); also summarized in Table B1). Land cover data are from NLCD (2019) and the
 319 Hydrologic Unit Code (HUC) classifications are sourced from USGS Watershed Boundary Dataset (2022).



320 assess the relative improvement of our 30 m Global Wetlands and Global NFWs dataset with the 500 m
321 Tootchi et al. (2019) data, we also contrasted the CW-WTD with the NLCD classes within the
322 verification watersheds. For equal comparisons, following Tootchi et al. (2019) we used the Messenger et
323 al. (2016) HydroLAKES to mask out large lake systems (≥ 10 ha) from both the Global Wetlands and the
324 NLCD data within the 21 verification watersheds.

325

326 2.4.3 Standard performance measures

327

328 We evaluated the floodplain and wetland spatial data within the 21 validation watersheds using
329 commonly employed performance measures. Following Wing et al. (2017), we first created a contingency
330 table for our performance assessment (Table 1). As noted, we selected 20 km^2 as the minimum
331 contributing area to develop stream networks in our global floodplain analysis, a reasonable area for flow-
332 accumulation that balances computational efficiency for global geospatial model development. Woznicki
333 et al. (2019), our benchmark floodplain dataset, used a 4.5 km^2 contributing area in their high-resolution
334 CONUS analysis. To appropriately compare between datasets of two varying resolutions, we removed
335 stream and river network components from the Woznicki et al. (2019) validation dataset developed with
336 contributing areas $< 20 \text{ km}^2$, as our model did not discern landscape data at that granularity.

337

338 **Table 1.** Contingency table of possible outcomes for each cell used in assessing the performance of either the
339 floodplain or wetland geospatially modeled data. We contrasted published benchmark data from Woznicki et al.
340 (2019) for floodplain extent against modeled GFPlain90 data. Wetland comparisons contrasted NLCD wetlands
341 (Dewitz, 2019, open water and wetland classes) against both Global Wetlands and Global NFWs data.

	Floodplain [or Wetland] in Benchmark data	Not Floodplain [or Wetland] in Benchmark data
Floodplain [or Wetland] in Modeled data	M_1B_1	M_1B_0
Not Floodplain [or Wetland] in Modeled data	M_0B_1	M_0B_0

342



343 To provide a full assessment of our geospatial modeling performance, we contrasted our GFPlain90
344 floodplain dataset across the 21 validation watersheds using the approaches described below following
345 Sampson et al. (2015), Wing et al. (2017), and others (e.g., Bates and De Roo, 2000; Alfieri et al., 2014;
346 Sangwan and Merwade, 2015; Jafarzadegan et al., 2018; Woznicki et al., 2019). We first contrasted our
347 GFPlain90 floodplains to Woznicki et al. (2019), our benchmark floodplain data. We then analyzed the
348 watershed-scale comparison of our Global Wetlands product versus the NLCD wetlands (combined open
349 water and wetland classes), our benchmark wetlands data. We followed with a comparison focusing only
350 on our Global NFWs data and those NLCD wetlands and open water pixels that were determined to be
351 non-floodplain systems (i.e., NLCD data that also do not overlap the GFPlain90 data nor coastal waters
352 and with lakes >10 ha removed). These NLCD wetlands were our benchmark non-floodplain wetland
353 data. Lastly, we assessed the mean and aggregate error bias of our analyses by exploring results at coarser
354 spatial granularity (i.e., 1 km pixel size) along the riverine network (for floodplain assessment) and, for
355 wetland metrics, throughout the entirety of our 21 performance assessment watersheds (Sampson et al.,
356 2015; Wing et al., 2017). The metrics described below were used in our analyses.

357

358 *Hit Rate* (Bates and De Roo, 2000; Horritt and Bates, 2002; Tayefi et al., 2007; Alfieri et al., 2014;
359 Sampson et al., 2015; Wing et al., 2017; Jafarzadegan et al., 2018) also referred to as Recall (Woznicki et
360 al., 2019) and Correct (Sangwan and Merwade, 2015), measures how well a geospatial model
361 classification replicates the benchmark data but does not penalize for overprediction. H varies from 0,
362 where there is no overlap between the modeled data and the benchmark data, to 1 where the modeled data
363 completely contain the benchmark data.

$$364 \quad \text{Hit Rate } (H) = \frac{M_1 B_1}{M_1 B_1 + M_0 B_1} \quad (1)$$

365

366 *Precision* (Woznicki et al., 2019), also known as Spatial Coincidence (Tootchi et al., 2019), indicates the
367 proportion of the benchmark data that are correctly predicted and mapped in the modeled data. This
368 metric, P , also ranges from 0 to 1 with higher values indicating better performance.



369
$$Precision (P) = \frac{M_1 B_1}{M_1 B_1 + M_1 B_0} \quad (2)$$

370

371 The *False Alarm Ratio* (Sampson et al., 2015; Wing et al., 2017) also known as the False Discovery
372 Ratio, quantifies modeled data overprediction relative to the benchmark data. F varies from 0 (zero false
373 alarms) to 1 (all false alarms); lower values are considered better performance. The False Alarm Ratio can
374 also be calculated as $1 - Precision$ (Woznicki et al., 2019).

375
$$False Alarm Ratio (FA) = \frac{M_1 B_0}{M_1 B_0 + M_1 B_1} \quad (3)$$

376

377 The *Critical Success Index* (CSI, Bates and De Roo, 2000; Aronica et al., 2002; Werner et al., 2005;
378 Fewtrell et al., 2008; Alfieri et al., 2014; Sampson et al., 2015; Wing et al., 2017), also known as
379 Jaccard's Index (Tootchi et al., 2019), and Fit (Sangwan and Merwade, 2015), penalizes for both over-
380 and under-prediction, ranging from 0 (no match) to 1 (perfect match).

381
$$Critical Success Index (CSI) = \frac{M_1 B_1}{M_1 B_1 + M_0 B_1 + M_1 B_0} \quad (4)$$

382

383 Woznicki et al. (2019) utilized a performance metric, $F1$, which combines the *Hit Rate* (called Recall by
384 Woznicki et al. 2019) and *Precision* using their harmonic mean. $F1$ also varies from 0 to 1, with higher
385 values indicating better performance.

386
$$F1 = 2 \left(\frac{H \times P}{H + P} \right) \quad (5)$$

387

388 *Error Bias* (EB) characterizes the tendency of the model towards under- or over-prediction (Sampson et
389 al., 2015). Values of 1 indicate no bias, $0 \leq EB < 1$ indicates underprediction whereas $1 < EB \leq \infty$
390 indicates the model is tending towards overprediction.

391
$$Error Bias (EB) = \frac{M_1 B_0}{M_0 B_1} \quad (6)$$

392

393 Lastly, two additional metrics were calculated that assessed performance at the 30 arc-sec (~1 km) scale.
394 These measures, *Mean Absolute Error* and *Aggregate Error Bias* (Sampson et al., 2015; Wing et al.,



395 2017), characterize the data accuracy across large spatial extents. Large spatial extents are areas where 30
396 m data and overlap accuracy is less a concern than general dataset performance for broad-scale end-user
397 applications (e.g., when coarser, watershed-scale “lumped” hydrologic characterizations of water storage
398 are all that is required). For these metrics, both estimated and benchmark data were resampled to 1 km
399 resolution across the whole of each watershed; values within each 1 km pixel ranged from 0 to 1 and
400 represented the fraction of the 30 m resolution estimates and benchmark data. We assessed floodplain
401 estimates after calculating the fractional abundance comprising each 1 km² pixel within a 1 km buffer
402 around the Woznicki et al. (2019) floodplain data. We additionally analyzed all wetlands at the
403 watershed-scale as well as focusing on non-floodplain wetlands (e.g., wetlands exclusive of the
404 GFPlain90 floodplain or coastal connections, our target aquatic system).

405
$$\text{Mean Absolute Error } (E_A) = \frac{\sum_{i=1}^N |M-B|}{N} \quad (7)$$

406

407
$$\text{Aggregate Error Bias } (B_A) = \frac{\sum_{i=1}^N M-B}{N} \quad (8)$$

408

409 Where M is the area estimated as floodplain (or wetland), B is the benchmark floodplain (or wetland)
410 area, and N is the number of 1 km cells with data. *Mean Absolute Error* and *Aggregate Error Bias* were
411 calculated for each of the 21 HUCs, following Wing et al. (2017).

412

413



414 **3 Results**

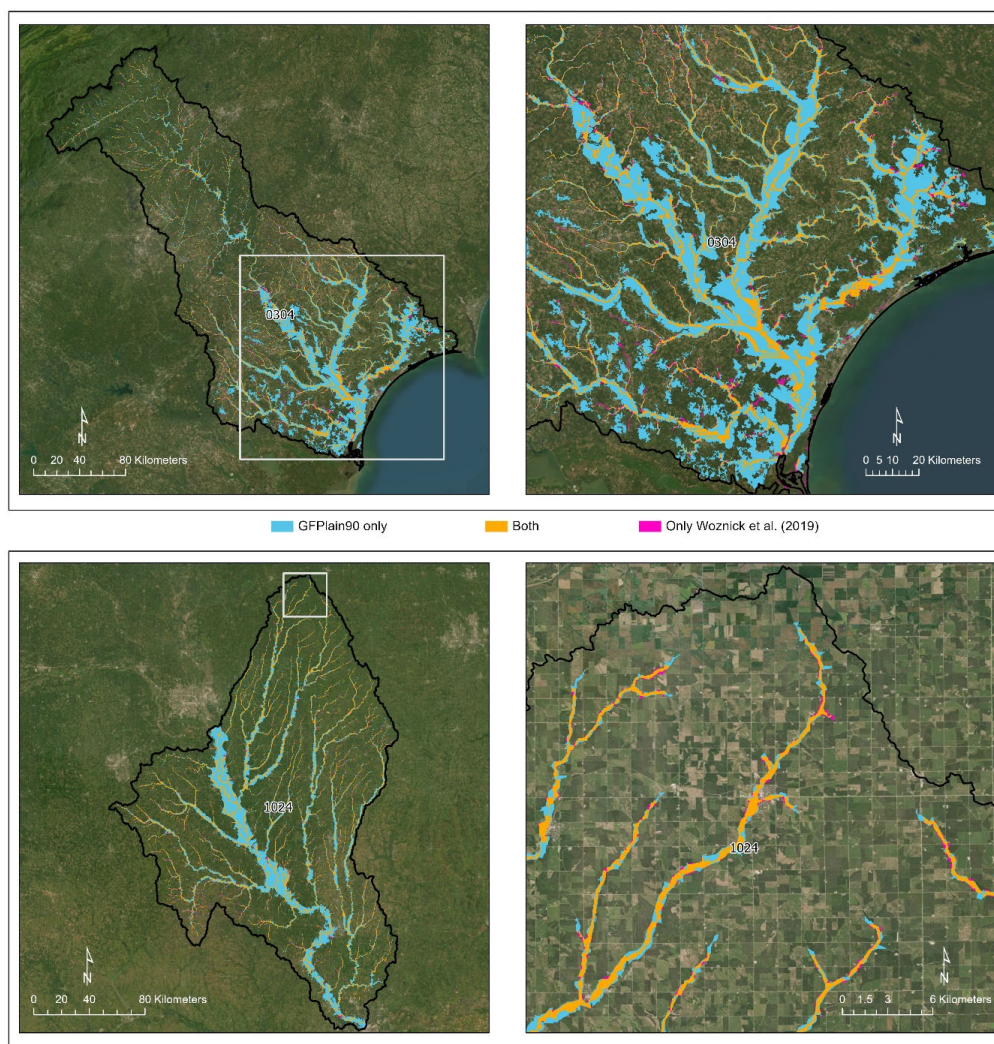
415

416 **3.1 Floodplain data performance**

417

418 The GFPlain90 floodplain data (Fig. 3) performed well when contrasted with the 100 yr coastal and
419 fluvial floodplain extent data from Woznicki et al. (2019), even though our analyses do not map coastal
420 floodplains. A median Hit Rate of 0.77 suggests that nearly 80% of the benchmark floodplain from
421 Woznicki et al. (2019) was similarly captured by the GFPlain90 floodplain data (Table 2). In addition, the
422 median False Alarm of 0.26 indicates that for every three pixels correctly identified as within the
423 Woznicki et al. (2019) floodplain, one pixel was incorrectly identified as such (i.e., a commission error
424 measure); this is evident in wider GFPlain90 floodplains in lower river reaches than predicted by
425 Woznicki et al. (2019). These performance values are similar to those reported by Woznicki et al. (2019,
426 False Alarm 0.22) and Wing et al. (2017, False Alarm 0.34-0.37). Critical Success Index (CSI) scores
427 penalize for over-prediction; our median value of 0.53 approximates previously published regional (e.g.,
428 Sangwan and Merwade, 2015, CSI values ranging from 0.44-0.89) and continental flood-extent
429 approaches (e.g., Sampson et al., 2015, CSI values from 0.43-0.67; Wing et al., 2017; CSI values between
430 0.50 and 0.55 reported). Median Precision (0.74) and F1 (0.70) values approximate those in the literature
431 as well (e.g., Woznicki et al., 2017 reported values of 0.78 for both). Mean Absolute Error of 0.08
432 reported here indicates an approximate 8 % difference between our GFPlain90 model and that of
433 Woznicki et al. (2017) at the 1 km cell resolution.

434



435

436 **Figure 3.** The robust performance of GFPlain90 relative to the benchmark Woznicki et al. (2019) floodplain data is
437 evident in the two rows, with the top panels (HUC_0304) a coastal watershed spanning North and South Carolina,
438 USA, and the bottom two panels different spatial extents of a midwestern USA watershed (HUC_1024). The
439 mainstem of the river network appeared wider in the GFPlain90 data in both examples, especially in the lower
440 reaches, though the complete network was well represented (i.e., floodplains were identified to the furthest extent of
441 the stream network's headwaters). Satellite imagery are sourced from ESRI (2022).



442 **Table 2.** Floodplain performance assessment of the GFPlain90-derived floodplain and the benchmark floodplain
 443 from Woznicki et al. (2019). The first six equations directly assess the spatial concordance and overlap between the
 444 two datasets, whereas Mean Absolute Error (Eq. 7) and Aggregate Error Bias (Eq. 8) are coarser fractional analyses
 445 (i.e., the fraction of a 1 km² cell predicted correctly) as measured along the riverine network.

Hydrologic Unit Code (HUC) ID	Hit Rate	Precision	False Alarm	CSI	F1	Error Bias	Mean Absolute Error	Aggregate Error Bias
	(Eq. 1)	(Eq. 2)	(Eq. 3)	(Eq. 4)	(Eq. 5)	(Eq. 6)	(Eq. 7)	(Eq. 8)
HUC_0101	0.76	0.84	0.16	0.66	0.80	0.62	0.06	-0.01
HUC_0103	0.92	0.77	0.23	0.72	0.84	3.25	0.05	0.03
HUC_0106	0.78	0.74	0.26	0.62	0.76	1.24	0.10	-0.03
HUC_0203	0.47	0.58	0.42	0.35	0.52	0.66	0.25	-0.18
HUC_0208	0.64	0.73	0.27	0.52	0.68	0.67	0.13	-0.08
HUC_0304	0.63	0.81	0.19	0.55	0.71	0.41	0.06	0.00
HUC_0313	0.62	0.72	0.28	0.50	0.67	0.62	0.09	-0.01
HUC_0501	0.77	0.85	0.15	0.68	0.81	0.59	0.04	-0.02
HUC_0706	0.86	0.79	0.21	0.69	0.82	1.62	0.04	0.02
HUC_0804	0.75	0.83	0.17	0.65	0.79	0.64	0.08	-0.02
HUC_1003	0.85	0.42	0.58	0.39	0.56	7.70	0.11	0.09
HUC_1015	0.81	0.74	0.26	0.63	0.78	1.54	0.06	0.02
HUC_1016	0.89	0.36	0.64	0.35	0.52	14.79	0.18	0.17
HUC_1024	0.90	0.88	0.12	0.80	0.89	1.19	0.03	0.00
HUC_1029	0.84	0.87	0.13	0.75	0.85	0.82	0.04	-0.01
HUC_1304	0.66	0.74	0.26	0.53	0.70	0.67	0.07	-0.01
HUC_1601	0.92	0.55	0.45	0.52	0.69	9.47	0.10	0.08
HUC_1708	0.60	0.71	0.29	0.48	0.65	0.60	0.08	-0.03
HUC_1711	0.70	0.50	0.50	0.41	0.58	2.25	0.10	-0.02
HUC_1805	0.59	0.59	0.41	0.41	0.59	1.00	0.14	-0.05
HUC_1808	0.98	0.44	0.56	0.44	0.61	82.97	0.24	0.23
Median	0.77	0.74	0.26	0.53	0.70	1.00	0.08	-0.01
Mean	0.76	0.69	0.31	0.56	0.71	6.35	0.10	0.01

446

447

448 3.2 Wetland data performance

449

450 3.2.1 Global Wetland dataset

451



452 The novel ensemble Global Wetlands approach improved upon the previously published Tootchi et al.
453 (2019) research product, the CW-WTD (Table 3) when contrasted with CONUS data. A median Hit Rate
454 value of 0.24 indicates that both the inclusive Global Wetlands and CW-WTD captured ~one-quarter of
455 the high-resolution, 30-m pixel size NLCD wetlands and open waters in the validation dataset. However,
456 across the 21 validation watersheds the Global Wetlands dataset developed here correctly identified more
457 wetlands than the CW-WTD alone, as indicated by an 8% mean increase in Precision, 43 % increase in
458 Critical Success Index, 38 % increase in F1, a -8 % decrease in the False Alarm ratio, and a 21 %
459 decrease in Error Bias. At coarser, 1 km² scales, there was a slight decrease in the Mean Absolute Error
460 associated with the Global Wetlands, and no difference in Aggregate Error Bias between the data
461 products.

462

463 **3.2.2 Global Non-Floodplain Wetland (Global NFW) dataset**

464

465 Non-floodplain wetland identification using the Global Wetlands data (i.e., Global NFWs) similarly
466 improved upon the CW-WTD product (Fig. 4). For instance, though the Hit Rate values were low (e.g.,
467 median values ≤ 0.10), underscoring both the difficulty in mapping non-floodplain wetlands and the
468 challenge of assessing performance using high-resolution data, Global NFW analyses correctly identified
469 50 % more non-floodplain wetlands than the CW-WTD (Table 4, Tootchi et al., 2019). Improvements
470 when focusing on non-floodplain wetlands were found in every category with the Global NFWs dataset,
471 demonstrating increased non-floodplain wetland accuracy versus the original CW-WTD across the
472 median metric values for Precision, Critical Success Index, F1, False Alarms, and Error Bias (e.g., 33 %
473 increase in Precision, 20 % increase in Critical Success Index, 10 % increase in F1 scores, and a 12 %

474

475

476



477 **Table 3.** Spatial performance assessment of both the Global Wetland (abbreviated here as GW) and CW-WTD
 478 (abbreviated here as WTD, Tootchi et al., 2019) datasets when contrasted with the benchmark NLCD wetlands
 479 (Dewitz, 2019). The first six equations directly assess the spatial concordance and overlap between each spatial
 480 dataset and the benchmark (e.g., CW-WTD contrasted with the NLCD), whereas Mean Absolute Error (MAE, Eq.
 481 7) and Aggregate Error Bias (AEB, Eq. 8) are coarser fractional analyses measured throughout each watershed (e.g.,
 482 the proportional abundance NLCD within each 1 km² cell is contrasted with the proportional abundance of Global
 483 Wetlands predicted correctly within that cell).

Hydrologic Unit Code (HUC) ID	Hit Rate		Precision		False Alarm		Critical Success	
	(Eq. 1)		(Eq. 2)		(Eq. 3)		(Eq. 4)	
	WTD	GW	WTD	GW	WTD	GW	WTD	GW
HUC_0101	0.31	0.32	0.51	0.53	0.49	0.47	0.24	0.25
HUC_0103	0.26	0.28	0.42	0.45	0.58	0.55	0.19	0.21
HUC_0106	0.25	0.27	0.41	0.44	0.59	0.56	0.18	0.20
HUC_0203	0.12	0.12	0.51	0.53	0.49	0.47	0.11	0.11
HUC_0208	0.31	0.33	0.56	0.65	0.44	0.35	0.25	0.28
HUC_0304	0.42	0.43	0.65	0.69	0.35	0.31	0.35	0.36
HUC_0313	0.39	0.41	0.58	0.64	0.42	0.36	0.30	0.33
HUC_0501	0.15	0.17	0.57	0.64	0.43	0.36	0.14	0.15
HUC_0706	0.24	0.25	0.86	0.92	0.14	0.08	0.23	0.24
HUC_0804	0.45	0.46	0.70	0.75	0.30	0.25	0.38	0.40
HUC_1003	0.14	0.16	0.32	0.41	0.68	0.59	0.11	0.13
HUC_1015	0.25	0.40	0.17	0.42	0.83	0.58	0.12	0.26
HUC_1016	0.13	0.16	0.54	0.70	0.46	0.30	0.12	0.15
HUC_1024	0.10	0.10	0.67	0.75	0.33	0.25	0.09	0.10
HUC_1029	0.10	0.13	0.51	0.72	0.49	0.28	0.09	0.13
HUC_1304	0.02	0.02	0.44	0.52	0.56	0.48	0.02	0.02
HUC_1601	0.29	0.33	0.34	0.45	0.66	0.55	0.19	0.24
HUC_1708	0.24	0.24	0.48	0.49	0.52	0.51	0.19	0.20
HUC_1711	0.09	0.10	0.46	0.51	0.54	0.49	0.08	0.09
HUC_1805	0.14	0.15	0.62	0.64	0.38	0.36	0.13	0.13
HUC_1808	0.12	0.13	0.51	0.55	0.49	0.45	0.11	0.11
Median	0.24	0.24	0.51	0.55	0.49	0.45	0.14	0.20
Difference		0.00		0.04		-0.04		0.06
Change (%)		0.0		7.8		-8.2		42.9

484

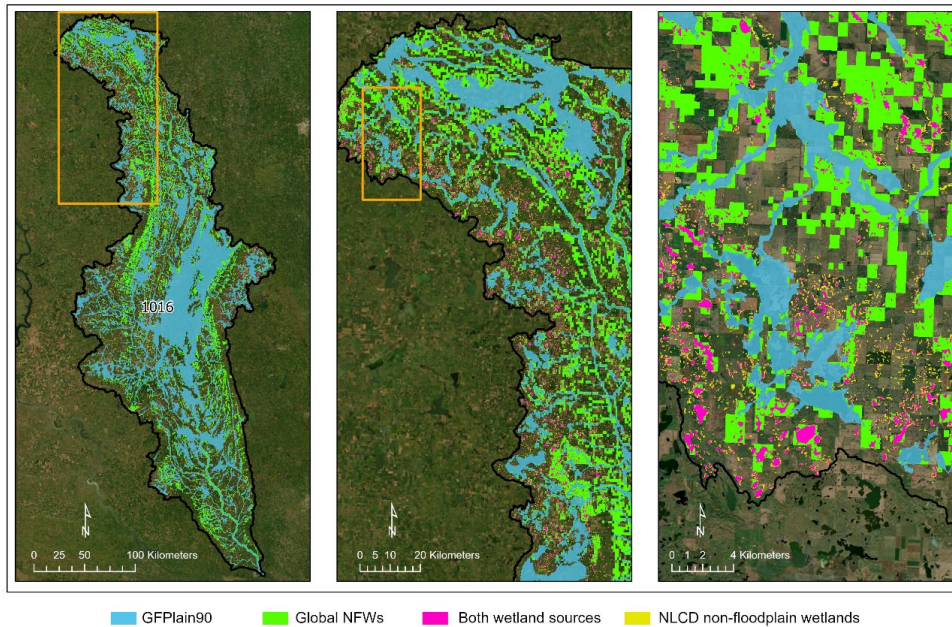


485 **Table 3.** (Continued)

Hydrologic Unit Code (HUC) ID	F1		Error Bias		MAE		AEB	
	(Eq. 5)		(Eq. 6)		(Eq. 7)		(Eq. 8)	
	WTD	GW	WTD	GW	WTD	GW	WTD	GW
HUC_0101	0.38	0.40	0.43	0.40	0.18	0.17	0.09	0.09
HUC_0103	0.32	0.34	0.50	0.47	0.16	0.15	0.06	0.07
HUC_0106	0.31	0.33	0.49	0.46	0.20	0.19	0.08	0.08
HUC_0203	0.19	0.20	0.13	0.13	0.36	0.36	0.28	0.28
HUC_0208	0.40	0.44	0.35	0.27	0.17	0.17	0.09	0.10
HUC_0304	0.51	0.53	0.39	0.34	0.21	0.21	0.12	0.13
HUC_0313	0.47	0.50	0.48	0.38	0.16	0.16	0.07	0.09
HUC_0501	0.24	0.26	0.14	0.11	0.10	0.10	0.09	0.09
HUC_0706	0.37	0.39	0.05	0.03	0.12	0.12	0.11	0.12
HUC_0804	0.55	0.57	0.36	0.29	0.20	0.20	0.12	0.14
HUC_1003	0.19	0.23	0.34	0.27	0.04	0.04	0.02	0.02
HUC_1015	0.21	0.41	1.59	0.91	0.05	0.04	-0.01	0.00
HUC_1016	0.21	0.26	0.13	0.08	0.26	0.26	0.23	0.24
HUC_1024	0.17	0.18	0.05	0.04	0.14	0.14	0.13	0.14
HUC_1029	0.17	0.22	0.11	0.06	0.11	0.12	0.10	0.11
HUC_1304	0.04	0.04	0.02	0.02	0.08	0.08	0.08	0.08
HUC_1601	0.31	0.38	0.80	0.59	0.05	0.05	0.01	0.01
HUC_1708	0.32	0.33	0.34	0.33	0.15	0.15	0.08	0.08
HUC_1711	0.15	0.17	0.12	0.11	0.17	0.17	0.14	0.15
HUC_1805	0.23	0.24	0.10	0.10	0.25	0.26	0.21	0.21
HUC_1808	0.20	0.20	0.13	0.12	0.09	0.09	0.07	0.07
Median	0.24	0.33	0.34	0.27	0.16	0.15	0.09	0.09
Difference		0.09		0.07		-0.01		0.00
Change (%)		37.5		-20.6		-6.3		0.0

486

487



488

489 **Figure 4.** Demonstration of the relative accuracy of the Global NFWs in identifying non-floodplain wetlands using a
490 Prairie Pothole Region watershed (HUC_1016, see Fig. 2) replete with abundant non-floodplain wetlands. Correctly
491 identified wetlands occur in both wetland sources (magenta color). Omission errors (NLCD non-floodplain
492 wetlands, smaller systems in yellow) and commission errors (Global NFWs, green) are evident as a result of the
493 higher resolution of the NLCD validation dataset. Satellite imagery are sourced from ESRI (2022).



494 **Table 4.** Non-floodplain wetland performance metrics contrasting both the Global NFWs (abbreviated here as
 495 GNFW) and CW-WTD (abbreviated here as WTD, Tootchi et al., 2019) non-floodplain wetland spatial data with the
 496 benchmark NLCD wetlands (Dewitz, 2019). Descriptions of the metrics are the same as in Table 3, though the focus
 497 here is on wetlands outside the GFPlain90-derived floodplain.

Hydrologic Unit Code (HUC) ID	Hit Rate		Precision		False Alarm		Critical Success Index	
	(Eq. 1)		(Eq. 2)		(Eq. 3)		(Eq. 4)	
	WTD	GNFW	WTD	GNFW	WTD	GNFW	WTD	GNFW
HUC_0101	0.24	0.25	0.43	0.45	0.57	0.55	0.18	0.19
HUC_0103	0.17	0.18	0.30	0.32	0.70	0.68	0.12	0.13
HUC_0106	0.15	0.18	0.14	0.17	0.86	0.83	0.08	0.10
HUC_0203	0.12	0.13	0.20	0.23	0.80	0.77	0.08	0.09
HUC_0208	0.14	0.16	0.34	0.41	0.66	0.59	0.11	0.13
HUC_0304	0.26	0.28	0.45	0.49	0.55	0.51	0.20	0.21
HUC_0313	0.21	0.23	0.35	0.40	0.65	0.60	0.15	0.17
HUC_0501	0.05	0.07	0.32	0.41	0.68	0.59	0.05	0.06
HUC_0706	0.05	0.06	0.63	0.72	0.37	0.28	0.05	0.05
HUC_0804	0.30	0.31	0.51	0.55	0.49	0.45	0.23	0.25
HUC_1003	0.04	0.07	0.13	0.21	0.87	0.79	0.03	0.05
HUC_1015	0.07	0.25	0.05	0.28	0.95	0.72	0.03	0.15
HUC_1016	0.07	0.11	0.31	0.53	0.69	0.47	0.06	0.10
HUC_1024	0.02	0.04	0.18	0.41	0.82	0.59	0.02	0.04
HUC_1029	0.03	0.06	0.25	0.58	0.75	0.42	0.03	0.06
HUC_1304	0.00	0.00	0.26	0.33	0.74	0.67	0.00	0.00
HUC_1601	0.05	0.09	0.07	0.16	0.93	0.84	0.03	0.06
HUC_1708	0.06	0.06	0.33	0.35	0.67	0.65	0.05	0.05
HUC_1711	0.04	0.05	0.22	0.27	0.78	0.73	0.04	0.05
HUC_1805	0.06	0.07	0.27	0.30	0.73	0.70	0.05	0.06
HUC_1808	0.05	0.06	0.25	0.36	0.75	0.64	0.04	0.06
Median	0.06	0.09	0.27	0.36	0.73	0.64	0.05	0.06
Difference		0.03		0.09		-0.09		0.01
Change (%)		50.0		33.3		-12.3		20.0

498

499



500 **Table 4.** (Continued)

Hydrologic Unit Code (HUC) ID	F1		Error Bias		Mean Absolute Error		Aggregate Error Bias	
	(Eq. 5)		(Eq. 6)		(Eq. 7)		(Eq. 8)	
	WTD	GFW	WTD	GFW	WTD	GFW	WTD	GFW
HUC_0101	0.31	0.32	0.41	0.39	0.16	0.16	0.08	0.09
HUC_0103	0.21	0.23	0.48	0.46	0.14	0.14	0.06	0.06
HUC_0106	0.14	0.18	1.11	1.03	0.11	0.11	-0.01	0.00
HUC_0203	0.15	0.17	0.53	0.51	0.09	0.09	0.03	0.03
HUC_0208	0.20	0.23	0.32	0.28	0.10	0.10	0.07	0.07
HUC_0304	0.33	0.35	0.44	0.40	0.17	0.17	0.08	0.09
HUC_0313	0.27	0.29	0.51	0.45	0.12	0.12	0.05	0.06
HUC_0501	0.09	0.11	0.12	0.10	0.09	0.09	0.07	0.08
HUC_0706	0.09	0.10	0.03	0.02	0.09	0.09	0.09	0.09
HUC_0804	0.38	0.40	0.43	0.37	0.13	0.13	0.07	0.07
HUC_1003	0.07	0.10	0.32	0.26	0.02	0.03	0.01	0.01
HUC_1015	0.06	0.26	1.46	0.85	0.03	0.02	-0.01	0.00
HUC_1016	0.11	0.19	0.17	0.11	0.15	0.15	0.12	0.13
HUC_1024	0.03	0.07	0.09	0.06	0.05	0.05	0.04	0.05
HUC_1029	0.05	0.11	0.09	0.05	0.08	0.08	0.07	0.07
HUC_1304	0.00	0.01	0.01	0.01	0.06	0.06	0.05	0.06
HUC_1601	0.05	0.11	0.68	0.50	0.02	0.02	0.00	0.01
HUC_1708	0.10	0.10	0.12	0.12	0.11	0.11	0.09	0.10
HUC_1711	0.07	0.09	0.16	0.15	0.09	0.09	0.07	0.07
HUC_1805	0.10	0.11	0.18	0.17	0.10	0.10	0.07	0.07
HUC_1808	0.08	0.11	0.15	0.12	0.02	0.02	0.01	0.01
Median	0.10	0.11	0.32	0.26	0.09	0.09	0.07	0.07
Difference		0.01		-0.06		0.00		0.00
Change (%)		10.0		-18.8		0.0		0.0

501

502 decrease in False Alarms and a 19 % decrease in Error Bias). There was no difference between the
 503 datasets with median values for Mean Absolute Error (median values for both = 0.09) or Aggregate Error
 504 Bias (median values for both = 0.07). Thus, at the 1 km² cell size, there was <10 % difference between
 505 both the CW-WTD and the Global NFWs and the benchmark NLCD non-floodplain wetlands and open
 506 waters (with the difference mostly stemming from an increase in identified wetlands with both CW-WTD
 507 and Global NFWs, as indicated with the positive Aggregate Error Bias values).

508



509 **3.3 Global extent analyses and synthesis**

510

511 **3.3.1 Floodplains**

512

513 Floodplains were estimated to cover 26.6 million km² (Table 5), or 19.7 % of the global landmass.
 514 Approximately 23-24 % of the African and Australasian land masses were categorized as occurring
 515 within a floodplain, the greatest percentage of global areas so categorized. Conversely, the Arctic
 516 (northern Canada and Alaska) and Greenland (excluding the ice sheet) had the least land mass categorized
 517 as floodplain (13-14 %). In comparison, Nardi et al. (2019) calculated a global floodplain extent of
 518 13,394,139 km², using a 250-m pixel size, a 1000 km² minimum contributing area, and bounding their
 519 study between 60°N and 60°S latitudes. Our analyses using the same latitudinal bounds but with a higher
 520 resolution dataset (90 m) and a 20 km² minimum contributing area identified 24,185,775 km², an 81 %
 521 areal increase (Fig. B1).

522

523 **Table 5.** Calculated floodplain area for each HydroBASINS at the global scale. Our analyses found 19.7 % of the
 524 landmass occurs within a floodplain.

HydroBASINS Region	Floodplain (km ²)	Floodplain Percent of Landmass
Africa	6,990,859	23.3 %
Arctic (northern Canada & Alaska)	894,594	14.2 %
Asia	4,283,991	20.6 %
Australasia	2,649,395	23.8 %
Europe and Middle East	3,415,308	19.1 %
Greenland (excl. ice sheet)	270,813	12.6 %
North & Central America (excl. Alaska)	2,713,346	17.0 %
Siberian Russia	2,051,305	15.8 %
South America	3,368,778	18.9 %
Total	26,638,389	19.7 %

525

526

527 **3.3.2 Wetlands**

528



529 Global Wetland extent covered 30.5 million km² (Table 6). With a focus on smaller systems compared to
 530 those presented by Tootchi et al. (2019), our Global Wetland dataset identified 11 % more potential
 531 global wetlands (3 million km² additional wetlands).

532

533 Australasia had the greatest proportional wetland abundance (see also Zhu et al., 2022), with wetlands
 534 covering 38 % of the landmass (driven, in part, by island abundance and fringing estuarine wetlands [Fan
 535 et al., 2013]). Greenland (3 %) and Africa (12 %) had the least wetlands identified on the land mass.

536

537 **Table 6.** Estimated Global Wetlands areal extent for each of the nine regional HydroBASINS (Lehner and Grill,
 538 2013). As described in the text, Global Wetlands extent incorporates the CW-WTD (Tootchi et al., 2019), CCI
 539 (Herold et al., 2015), and GSW (Pekel et al., 2016); lakes of ≥ 10 ha have been removed (Messenger et al., 2016).

HydroBASINS Region	Wetlands (km ²)	Wetland Percent of Landmass
Africa	3,524,917	11.8 %
Arctic (northern Canada & Alaska)	1,807,830	28.6 %
Asia	5,543,333	26.6 %
Australasia	4,283,996	38.4 %
Europe and Middle East	2,465,074	13.8 %
Greenland (excl. ice sheet)	60,761	2.8 %
North & Central America (excl. Alaska)	4,107,333	25.8 %
Siberian Russia	3,578,868	27.6 %
South America	5,140,139	28.8 %
Total	30,512,251	22.6 %

540

541

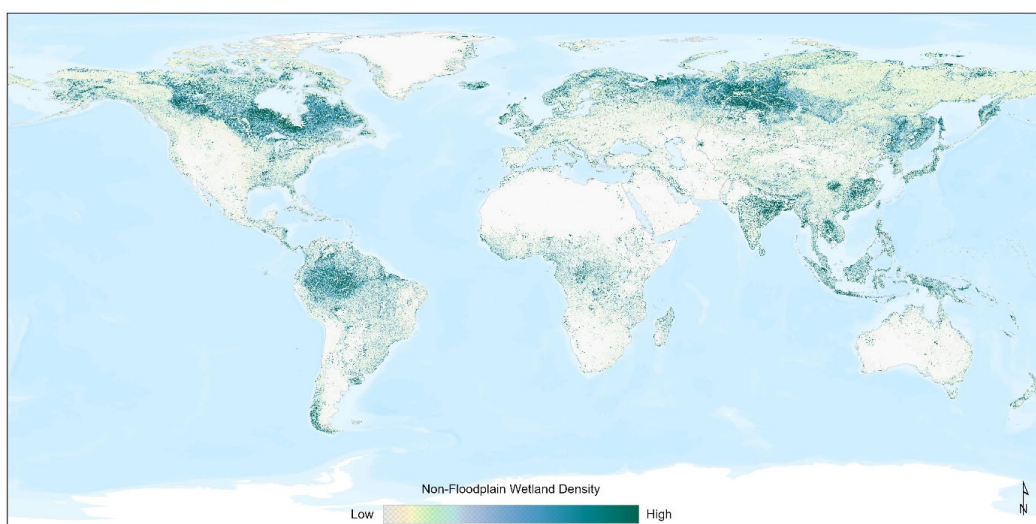
542 3.3.3 Non-floodplain wetlands (Global NFW)

543

544 Approximately 16.0 million km² of potential non-floodplain wetlands were identified globally (Global
 545 NFWs, Fig. 5), meaning that 11.9 % of the global landmass is estimated to be covered by non-floodplain
 546 wetlands (Table 7). This represents ~53 % of the total global wetlands found in the dataset used in this
 547 analysis (see Methods: Wetland Data, above). The global distribution of non-floodplain wetlands is
 548 widespread, though they were found to comprise a higher proportion of wetlands within more northern

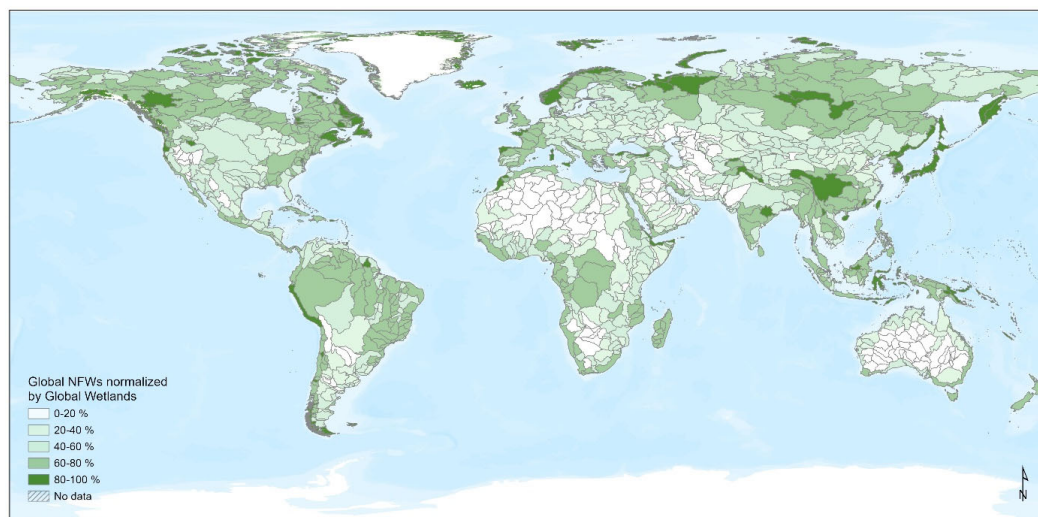


549 HydroBASINS watersheds (i.e., higher abundances in formerly glaciated basins), as demonstrated in Fig.
550 6. The Arctic portion of northern Canada and Alaska (21.7 %), and Siberian Russia (17.4 %), typically
551 underlain by permafrost and frequently inundated or saturated due to poor drainage evolution
552 (Kremenetski et al., 2003; Robarts et al., 2013; Olefeldt et al., 2021), had the greatest percent non-



553
554 **Figure 5.** Non-floodplain wetlands, Global NFWs, are found worldwide, with a greater abundance in formerly
555 glaciated landscapes of northern climates (e.g., northern North America and Siberian Russia) as well as within the
556 Amazon basin (South America). This density map was created using the Focal Statistics tool in ArcGIS Pro 2.9.1.
557 The basemap layer is the ESRI World Terrain Base (2022).

558
559
560



561

562 **Figure 6.** The proportion of non-floodplain wetlands, Global NFWs, within a given HydroBASINS watershed
563 (Lehrner and Grill, 2013), ranging up to 100 %, varied globally. The impacts or effects of non-floodplain wetlands
564 on biological, biogeochemical, and hydrological functions will vary based on their relative abundance, location
565 within the watershed, and hydrologic characteristics (Lane et al., 2018). The basemap layer is the ESRI World
566 Terrain Base (2022).

567

568

569 floodplain wetlands. Africa (5.4 %) and Greenland (1.0 %, excluding ice sheets) had the least abundance
570 of non-floodplain wetlands. A four-direction region-group (contagion) analysis conducted to identify
571 adjacent pixels considered as contiguous units or non-floodplain wetland systems identified 32.8 million
572 individual non-floodplain wetlands. Non-floodplain wetlands are typically small aquatic systems (see
573 Table 7): the median size differed across the HydroBASINS regions from 0.018 km² (1.8 ha) to 0.138
574 km² (13.8 ha) with a global median of 0.039 km² (3.87 ha).



575 **Table 7.** Global NFW data further described by HydroBASIN region.

HydroBASINS Region	Global NFW Extent (km ²)	Count of Global NFWs (#)	Global NFW Percent of Landmass	Global NFW Median Area (km ²)
Africa	1,611,225	2,698,465	5.4 %	0.138
Arctic (northern Canada & Alaska)	1,371,937	5,956,081	21.7 %	0.018
Asia	2,924,900	4,564,172	14.0 %	0.049
Australasia	850,402	1,448,315	7.6 %	0.054
Europe and Middle East	1,475,355	3,740,961	8.3 %	0.054
Greenland (excl. ice sheet)	21,747	180,726	1.0 %	0.018
North & Central America (excl. Alaska)	2,608,158	5,740,066	16.4 %	0.025
Siberian Russia	2,255,689	4,864,577	17.4 %	0.063
South America	2,891,604	3,572,294	16.2 %	0.096
Total	16,011,018	32,765,657	11.9 %	0.039

576

577 **4 Discussion**

578

579 We report here for the first time the global abundance of non-floodplain wetlands, a functionally
 580 important and imperiled resource (Creed et al., 2017). Our estimate of 16.0 million km² suggests that
 581 approximately 53 % of the global population of wetlands are likely non-floodplain wetland systems.
 582 These aquatic systems are small, with a range from 0.018-0.138 km² (1.8-13.8 ha) across the globe and a
 583 global median size of 0.039 km² (3.87 ha, see Table 7).

584

585 The global abundance of non-floodplain wetlands is a reasonable first approximation of the total non-
 586 floodplain wetland extent. For instance, non-floodplain wetland estimates in the CONUS were conducted
 587 by Lane et al. (2022) using high-resolution aerial-sourced spatial data layers developed by the National
 588 Wetlands Inventory (U.S. Fish and Wildlife Service, various dates). Lane et al. (2022) reported
 589 approximately 23% of the area of freshwater wetlands to be non-floodplain wetland systems. Yet the
 590 CONUS has lost nearly half of its wetlands since the European colonization (Dahl, 1990), with smaller
 591 and shallower non-floodplain wetlands likely being disproportionately lost (Van Meter and Basu, 2015;
 592 Serran et al., 2017).

593



594 Tootchi et al. (2019) – our base input geospatial data layer – calculated that the global wetland extent
595 identified from incorporating both regularly flooded wetland systems (surface-water and precipitation-
596 sourced) and groundwater-driven wetland systems (e.g., Fan et al., 2013; Hu et al., 2017b) resulted in
597 approximately 27.5 million km² of wetlands, a value towards the higher-end of previously published
598 geospatial wetland datasets (Hu et al., 2017a). In their synthesis, Tootchi et al. (2019) explained their
599 values as particularly influenced by groundwater-driven wetlands, especially those in the tropics (10° N-
600 10° S latitudes, Zhu et al., 2022), following recent studies acknowledging the under-estimation of those
601 wetland systems (e.g. Wania et al., 2013; Gumbricht et al., 2017).

602

603 It follows that incorporating additional higher-resolution satellite inundation data (Pekel et al., 2016) as
604 well as groundwater-driven wetland systems data (e.g., Fan et al., 2013; Tootchi et al., 2019), as
605 conducted in this study, would similarly maintain the trend towards the higher end in global estimates as
606 found by Hu et al. (2017a) and Tootchi et al. (2019). This is meted out in the simple contrast between the
607 proportional abundance of non-floodplain wetland systems identified here against the 30 m NLCD data
608 product described above (Dewitz, 2019) across the 21 CONUS watersheds in this study. The calculated
609 median watershed abundance of non-floodplain wetlands in both the Global NFWs (9.4 %) and the
610 Tootchi et al. (2019) CW-WTD (9.1 %) datasets from our validation watersheds are nearly 5-fold the
611 abundance of the benchmark data from the NLCD (Table 7). However, this is contrasted with a 7-fold
612 *under-representation* of non-floodplain wetlands as derived from the satellite based GSW data (Table 8,
613 Pekel et al., 2016).

614

615 It is apparent that the GSW alone is insufficient to map non-floodplain wetlands (this study, Vanderhoof
616 and Lane, 2019). Though useful as a satellite-based input data layer, the GSW by itself appears
617 inadequate for identifying non-floodplain wetlands because it relies on surface-water inundation and
618 ignores saturated wetland systems and those driven by groundwater discharge and upwelling (Winter et
619 al., 1998). Fan et al. (2013) found that groundwater drivers of aquatic system state were important and



620 **Table 8.** A comparison of the non-floodplain wetland distribution within the 21 HUCs contrasting across NLCD
 621 (the benchmark data layer, Dewitz, 2019), Global NFW (this study), CW-WTD (Tootchi et al., 2019), and GSW
 622 (Pekel et al., 2016). The CW-WTD (at 500 m) and the Global NFW (coupling 500 m, 300 m, and 30 m data),
 623 derived from the CW-WTD, identified 5-fold the abundance of non-floodplain wetlands whereas the GSW under-
 624 estimated non-floodplain wetlands nearly 7-fold.

HUC ID	Percent HUC as NLCD NFW	Percent HUC as Global NFW	Percent HUC as CW-WTD NFW	Percent HUC as GSW NFW
HUC_0101	10.4 %	19.2 %	18.9 %	0.1 %
HUC_0103	8.1 %	14.6 %	14.3 %	0.2 %
HUC_0106	8.2 %	8.0 %	7.5 %	0.3 %
HUC_0203	4.9 %	8.4 %	8.3 %	0.4 %
HUC_0208	4.7 %	12.0 %	11.5 %	4.6 %
HUC_0304	12.2 %	21.7 %	20.8 %	12.2 %
HUC_0313	8.3 %	14.4 %	13.5 %	8.2 %
HUC_0501	1.5 %	9.2 %	8.9 %	0.1 %
HUC_0706	0.7 %	9.7 %	9.5 %	0.3 %
HUC_0804	9.7 %	17.1 %	16.2 %	9.7 %
HUC_1003	0.7 %	2.1 %	1.9 %	0.2 %
HUC_1015	1.8 %	2.0 %	1.3 %	0.1 %
HUC_1016	3.6 %	16.6 %	15.5 %	2.6 %
HUC_1024	0.5 %	5.1 %	4.9 %	0.2 %
HUC_1029	0.9 %	8.4 %	7.7 %	0.4 %
HUC_1304	0.0 %	5.5 %	5.5 %	0.0 %
HUC_1601	0.7 %	1.3 %	1.0 %	0.1 %
HUC_1708	2.0 %	11.7 %	11.6 %	0.4 %
HUC_1711	1.8 %	9.4 %	9.1 %	0.2 %
HUC_1805	2.2 %	9.9 %	9.7 %	0.5 %
HUC_1808	0.3 %	1.7 %	1.6 %	0.1 %
Median	2.0 %	9.4 %	9.1 %	0.3 %

625
 626 underrepresented in global datasets. Relying on surface water inundation captured during satellite
 627 overflights depends not only on an unobstructed view of the waterbody (e.g., not obscured by trees) but
 628 also fortuitous timing regarding inundation status. For example, in an analysis of non-floodplain wetlands
 629 of the CONUS as derived by distance from an aquatic system, Lane and D’Amico (2016) reported that
 630 just over 50 % of the non-floodplain wetlands were classified as seasonally or temporarily flooded –
 631 meaning that cloud-free and unobscured overflights would only potentially identify these systems at
 632 certain inundated times of the year. Additionally, Lane and D’Amico (2016) identified another 6 % of
 633 CONUS non-floodplain wetlands as saturated (i.e., wetlands with saturated substrates but with surface
 634 water seldom present). These wetlands would not be identified by the GSW (Pekel et al., 2016) resulting



635 in a further under-representation of the global resource. Similarly, Hamunyela et al. (2022), analyzing
636 ~150,000 km² in southeastern Africa, found that the GSW underestimated surface water extent (i.e.,
637 omission errors) by nearly 65%. Vanderhoof and Lane (2019) found approximately 42% omission rates
638 when contrasting the GSW data to surface-water extent in non-floodplain wetlands ranging from 0.2-17.6
639 ha in area in the Midwestern US. While the GSW is an outstanding dataset that is continuing to be
640 managed and updated, the GSW and its derived product have limitations in their stand-alone utility in
641 global non-floodplain wetland analyses.

642

643 While solely using satellite-based surface-water data products omits groundwater-driven and saturated
644 wetlands and likely results in non-floodplain wetland underestimations, our Global Wetland data
645 incorporated the finer-resolution CCI (Herold et al., 2015) and GSW (Pekel et al., 2016) products into the
646 Tootchi et al. (2019) base map, substantially improving the identification of non-floodplain wetlands.
647 These improvements, as indicated by performance indices increasing from 10-50 % in the derived Global
648 Wetland data (see Table 4), support the inclusion of these higher-resolution satellite-based data (Herold et
649 al., 2015; Pekel et al., 2016) with groundwater datasets (Fan et al., 2013), especially when focused on
650 smaller and non-floodplain wetland systems. Similarly, at a coarser scale of 1 km, there was a difference
651 in Mean Absolute Error value of 0.09 (see Table 4) between the Global NFWs and the benchmark NLCD.
652 This ~9 % difference between the two datasets at a 1 km resolution (the former originating at 500 m and
653 the latter at 30 m) further suggest substantive potential utility in these global non-floodplain wetland data
654 for effective natural resource management and decision-making.

655

656



657 **5 Implications**

658

659 Non-floodplain wetlands remain vulnerable waters (Creed et al., 2017), despite the fact that the
660 hydrological, biogeochemical, and biological functions performed by non-floodplain wetlands are
661 increasingly noted in the literature (e.g., Leibowitz, 2003; Creed et al., 2017; Lane et al., 2018; Lane et
662 al., 2022), incorporated into eco-hydrological models by the scientific community (e.g., Fossey and
663 Rousseau, 2016; Golden et al., 2017; Golden et al., 2021; Leibowitz et al., In Review), and considered by
664 policy makers (e.g., Biggs et al., 2017; Drenkhan et al., 2022). Their global fate has important
665 implications for watershed-scale resilience to changing climatic conditions (Mckenna et al., 2017; Lane et
666 al., 2022) affecting the measured benefits humans receive from biogeochemical processing, stormwater
667 attenuation, and drought mitigation functions provided by non-floodplain wetlands.

668

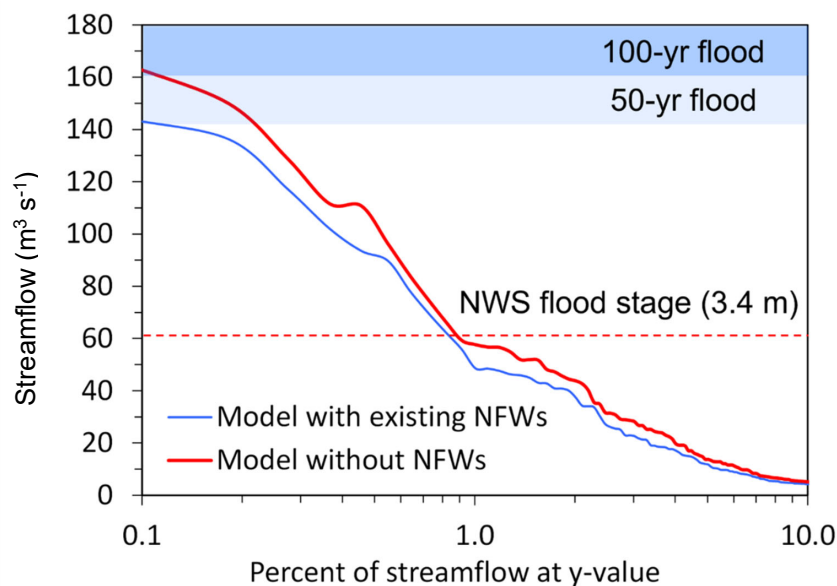
669 Global attention to functions of non-floodplain wetlands has increased in the United States (Marton et al.,
670 2015; Rains et al., 2016; Cohen et al., 2016), Europe (Biggs et al., 2017; Nitzsche et al., 2017; Rodríguez-
671 Rodríguez et al., 2021), Asia (Kam, 2010; Van Meter et al., 2014), Australia (Adame et al., 2019), Africa
672 (Merken et al., 2015; Samways et al., 2020), South America (Rodrigues et al., 2012; Cunha et al., 2019)
673 and elsewhere (see extensive review in Chen et al., 2022). This includes analyses of non-floodplain
674 wetlands both as individual systems (e.g., assessing the functions of a single wetland or wetland complex;
675 Badiou et al., 2018) as well as agglomerated, watershed-scale functioning systems (e.g., answering
676 questions on the functional contributions of all non-floodplain wetlands at larger spatial extents; Golden
677 et al., 2016; Blanchette et al., 2022). Previous studies found that non-floodplain wetlands are
678 overwhelmingly important contributors to biogeochemical and hydrological functions affecting
679 downgradient (i.e., down-stream) water quality and streamflow (e.g., McLaughlin et al., 2014; Marton et
680 al., 2015; Cohen et al., 2016; Rains et al., 2016; Golden et al., 2019; Cheng et al., 2020). Hence, with the
681 development of this publicly available dataset, and subsequent improvements by others, it is hoped that



682 these important aquatic systems will be incorporated into resource management and decision-making
683 across the globe.

684

685 Recently, Lane et al. (2022) identified global-scale geospatial data of the spatial extent and spatial
686 configuration of vulnerable waters – non-floodplain wetlands and headwater stream systems (e.g.,
687 ephemeral, intermittent, and perennial low-order waters [Strahler, 1957]) – as a critical scientific gap.
688 Discounting their significance in watershed-scale hydrology and nutrient biogeochemistry analyses – as
689 well as their importance in biological processes (Schofield et al., 2018; Smith et al., 2019; Mushet et al.,
690 2019) – affects quantification of the myriad ecosystem services they provide (De Groot, 2006; Colvin et
691 al., 2019). For instance, Golden et al. (2021) provide a tangible example of the functional effects and
692 influence of non-floodplain wetlands once incorporated into watershed-scale hydrologic models (Fig. 7):
693 ignoring non-floodplain wetlands in the model resulted in projected critical flood-stage return intervals
694 (e.g., 50 yr and 100 yr floods) being reached within a given modeled time frame. Conversely,
695 incorporating non-floodplain wetlands and their storage capacities into a river basin model (e.g., Rajib et
696 al., 2020) demonstrated that non-floodplain wetlands significantly attenuate storm flows, for when non-
697 floodplain wetlands are “...integrated into the model, those simulated *flood stages are not reached*”
698 (Golden et al., 2021, p. 3, emphasis added). The hydrological functions and concomitantly the associated
699 biogeochemical functions (e.g., Marton et al., 2015) of non-floodplain wetlands demand an effective
700 accounting of their spatial extent and configuration, as demonstrated in this novel global dataset.



701

702 **Figure 7.** Non-floodplain wetlands attenuate storm flows and decrease flooding hazards. In this example from
703 Golden et al. (2021, used by permission), incorporating the floodwater storage and attenuation functions of non-
704 floodplain wetlands (NFWs, here) resulted in substantive decreases in flood-stage heights (i.e., modeled stream
705 outcomes incorporating non-floodplain wetlands reached neither 50 yr nor 100 yr floods extents). The example from
706 Golden et al. (2021) is of USGS Pipestem Creek gage 06469400, draining approximately 1,800 km².

707

708 **6 Global Non-Floodplain Wetlands: Continuing advancements and conclusion**

709

710 Noting the challenges in accurately identifying non-floodplain wetlands – including small size, frequent
711 non-perennial hydrological inundation, soil saturation rather than overlying surface water, and canopy or
712 cloud cover obstructing satellite or airborne detection – recommendations for advanced analyses of non-
713 floodplain wetland extent hinge initially on the use of ancillary data sources. For instance, global
714 assessments will be improved through wall-to-wall high resolution digital elevation models that are used
715 to identify depressions on the landscape (e.g., Wu et al., 2019b). Though not all landscape depressions are
716 non-floodplain wetlands (or wetlands at all), analyses that include depressions may find improved



717 performance when used in combination with vegetation-based assessments or spectral analyses
718 identifying water (Devries et al., 2017; Evenson et al., 2018b). Similarly, emerging synthetic aperture
719 radar-based landscape classifications (e.g., Huang et al., 2018; Martinis et al., 2022; Brown et al., 2022)
720 and both airborne and satellite-borne hyperspectral and advanced analyses, including LiDAR, as well as
721 analytical capabilities (e.g., machine-learning approaches, object-oriented classifications, Berhane et al.,
722 2018); topographically based models, Xi et al., 2022) hold great promise for improved resolution and
723 performance in identifying non-floodplain wetlands (Christensen et al., 2022).

724

725 The keys to quantifying the functional contributions, ecosystem services, and watershed-scale resilience
726 conferred by non-floodplain wetlands through hydrological, biogeochemical, and biological processes are
727 found through, as a first principle, identifying the spatial extent and configuration of this disappearing and
728 imperiled aquatic system (Creed et al., 2017; Lane et al., 2022). This novel geospatial dataset, freely
729 available (https://gaftp.epa.gov/EPADDataCommons/ORD/Global_NonFloodplain_Wetlands/, Lane et al.,
730 2023), provides for sustainable management of an important aquatic resource and advances the global
731 assessment of non-floodplain wetland functions by facilitating non-floodplain wetland inclusion in both
732 existing models and those under development (Golden et al., 2021).

733

734 **7 Data availability**

735

736 The data are available on the United State Environmental Protection Agency's Environmental Dataset
737 Gateway (DOI: <https://doi.org/10.23719/1528331>, Lane et al., 2023) or
738 https://gaftp.epa.gov/EPADDataCommons/ORD/Global_NonFloodplain_Wetlands/, (last accessed
739 12/06/2022). Here, we provide global gridded floodplain (90 m, GFPLain90, ~/Global_Floodplains),
740 global gridded wetlands (30 m, Global Wetlands, ~/Global_Wetlands), and global gridded non-floodplain
741 wetlands (30 m, Global NFWs, ~/Global_NFWs) for each of the 3142 HydroBASINS, organized by
742 HydroBASINS region (see, e.g., Table 7).



743

744 **Author contributions.** CL, JC, HG, and ED conceptualized the study, developed the formal analysis, and
745 conducted and/or assisted the data validation. CL wrote and edited the manuscript, while JC and HG
746 reviewed and edited the manuscript. ED also developed the methodology, curated the data, conducted the
747 formal spatial analysis, validated the data, visualized the data, and reviewed and edited the manuscript.
748 QW and AR assisted in methodology development, validated the study outputs, conducted formal
749 analyses, and reviewed and edited the manuscript.

750

751 **Competing interests.** The corresponding authors have declared that none of the authors have any
752 competing interests.

753

754 **Disclaimer.** Publisher's note: Copernicus Publications remains neutral with regard to jurisdictional
755 claims in published maps and institutional affiliations.

756

757 **Acknowledgements.** We greatly appreciate the scientific contributions and stimulative discussions in the
758 papers led by Ardalan Tootchi, Sean Woznicki, Fernando Nardi, Oliver Wing, Paul Bates, and their co-
759 authors that inspired us to complete these analyses. Jeremy Baynes and John Johnston conducted critical
760 reviews to improve this manuscript, and their efforts are acknowledged. This paper has been reviewed in
761 accordance with the US Environmental Protection Agency's peer and administrative review policies and
762 approved for publication. Mention of trade names or commercial products does not constitute
763 endorsement or recommendation for use. Statements in this publication reflect the authors' professional
764 views and opinions and should not be construed to represent any determination or policy of the US
765 Environmental Protection Agency.

766

767 **Review statement.** This paper was edited by [Topical Editor] and reviewed by [names/anonymous].

768



769 **Appendix A: Abbreviations**

770	AEB	Aggregate error bias
771	CCI	Climate change initiative
772	CONUS	Conterminous United States
773	CSI	Critical Success Index
774	CW-WTD	Composite wetland-water table depth
775	DEM	Digital elevation model
776	EB	Error Bias
777	EPA	Environmental Protection Agency
778	ESA	European Space Agency
779	FA	False Alarm
780	FEMA	Federal Emergency Management Agency
781	GDW	Groundwater-driven wetlands
782	GFPlain	Global Floodplain
783	GIEMS-D15	Global Inundation Extent from Multi-Satellites Downscaled - 15 arcseconds
784	GIS	Geographic information systems
785	GLWD	Global Lakes and Wetlands Database
786	GNFW	Global Non-floodplain wetlands
787	GSW	Global surface water
788	GW	Global wetlands
789	H	Hit Rate
790	HUC	Hydrologic unit code
791	IPCC	Intergovernmental Panel on Climate Change
792	LIDAR	Light detection and ranging
793	MAE	Mean absolute error
794	MERIT	Multi-Error Removed Improved Terrain



795	ML	Machine learning
796	NFW	Non-floodplain wetland
797	NLCD	National Land Cover Database
798	NWS	National Weather Service
799	P	Precision
800	RFW	Regularly flooded wetland
801	SAR	Synthetic aperture radar
802	USA	United States of America
803	USGS	United States Geological Survey
804	UTM	Universal Transverse Mercator
805	WTD	Water table depth
806		



807 **Appendix B: Supplemental Tables and Figures**

808

809 **Table B1.** Descriptive characteristics of the 21 verification basins located throughout the CONUS (see Fig. 2).
 810 Majority Köppen-Geiger classification follows Beck et al. (2018). Climatological data were acquired from the
 811 PRISM Climate Group (Parameter-elevation Regressions on Independent Slopes Model, prism.oregonstate.edu/,
 812 accessed 09/26/2022) using the 30-year annual normals for each watershed. Land use data and descriptions are from
 813 the 2019 NLCD (www.mrlc.gov/data, accessed 09/26/2022) and represent the land use class with the greatest areal
 814 abundance. Average elevation was derived from the USGS National Elevation Dataset (https://www.usgs.gov/3d-
 815 elevation-program, accessed 01/13/2022). Global Wetland Count are the counts of wetlands from the derived Global
 816 Wetland database within each watershed after region-grouping the data using a four-direction contagion criterion
 817 (i.e., pixels immediately adjacent in any of the four cardinal directions are considered part of a unique, multi-pixel
 818 wetland, ArcGIS Pro v.2.9.1, Redlands, California).

Hydrologic Unit Code	Area	Köppen-	Mean Annual	Mean Annual
ID	(km ²)	Geiger	Temp (°C)	Rainfall (m)
HUC_0101	18,906	Dfb	4.0	1.1
HUC_0103	15,287	Dfb	5.4	1.2
HUC_0106	10,800	Dfb	7.5	1.3
HUC_0203	12,490	Dfa	11.6	1.2
HUC_0208	47,449	Cfa	13.7	1.2
HUC_0304	47,899	Cfa	16.4	1.3
HUC_0313	52,169	Cfa	18.1	1.4
HUC_0501	30,371	Dfb	8.6	1.2
HUC_0706	22,257	Dfa	8.1	1.0
HUC_0804	53,108	Cfa	17.5	1.4
HUC_1003	51,431	BSk	5.6	0.4
HUC_1015	37,098	Dfa	8.7	0.5
HUC_1016	54,743	Dfa	6.4	0.6
HUC_1024	35,237	Dfa	10.8	0.9
HUC_1029	48,204	Dfa	13.2	1.1
HUC_1304	48,126	BSh	18.6	0.4
HUC_1601	19,463	BSk	5.7	0.5
HUC_1708	16,101	Csb	9.0	2.1
HUC_1711	35,651	Csb	8.2	2.0
HUC_1805	11,341	Csb	14.9	0.7
HUC_1808	11,789	BSk	8.4	0.4



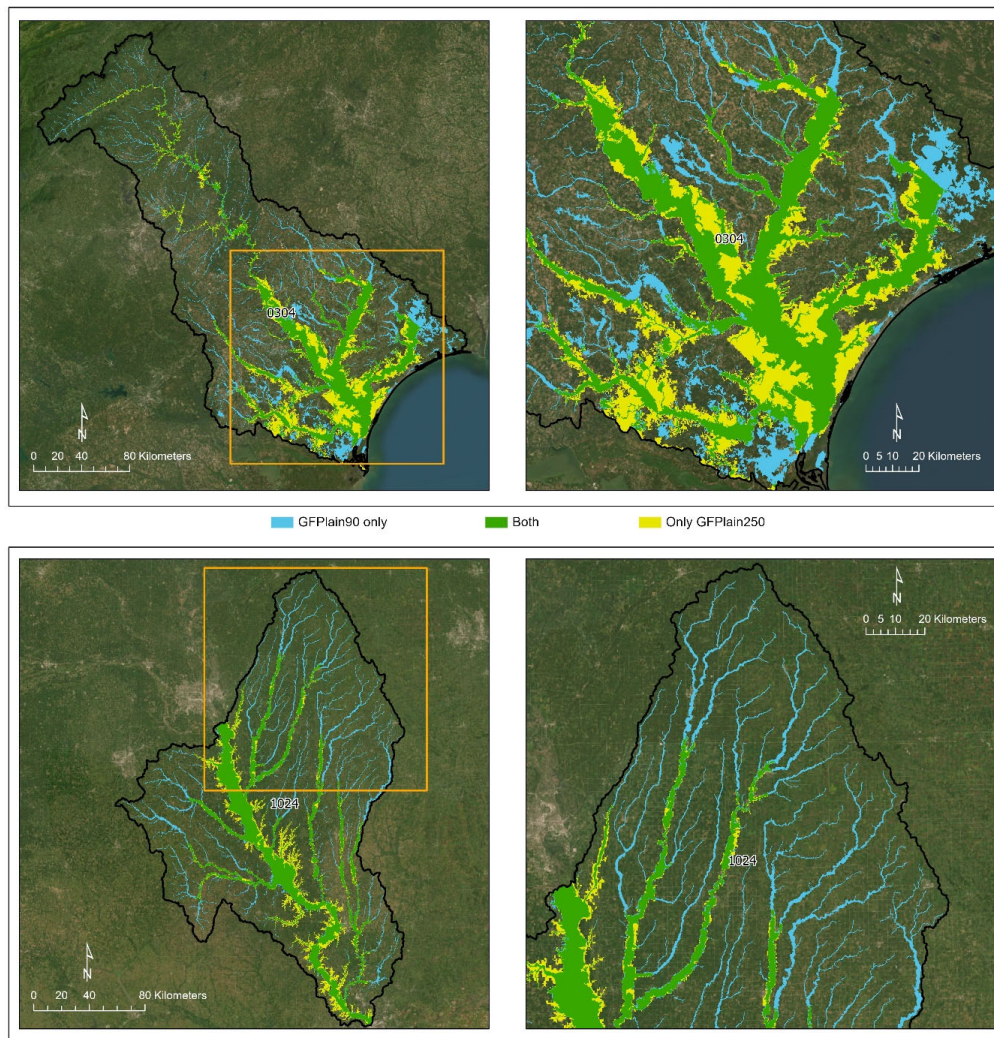
819 † Köppen-Geiger Class Descriptions (Beck et al. 2018): BSh (arid, steppe, hot), BSk (arid, steppe, cold), Cfa
 820 (temperate, no dry season, hot summer), Csb, (temperature, dry season, warm summer), Dfa (cold, no dry season,
 821 hot summer), Dfb (cold, no dry season, warm summer)

822

823 **Table B1.** (Continued)

Hydrologic Unit	Majority Land	Majority Land	Global Wetland	Average
Code	Use Coverage	Coverage Description	Count	Elevation
HUC_0101	43	Mixed Forest	2,141	296
HUC_0103	43	Mixed Forest	2,202	300
HUC_0106	43	Mixed Forest	2,799	169
HUC_0203	41	Deciduous Forest	2,438	82
HUC_0208	41	Deciduous Forest	13,934	187
HUC_0304	90	Woody Wetlands	14,643	127
HUC_0313	42	Evergreen Forest	27,056	147
HUC_0501	41	Deciduous Forest	6,310	484
HUC_0706	82	Cultivated Crops	3,100	300
HUC_0804	42	Evergreen Forest	12,242	85
HUC_1003	71	Herbaceous	11,852	1349
HUC_1015	71	Herbaceous	8,628	961
HUC_1016	82	Cultivated Crops	61,482	464
HUC_1024	82	Cultivated Crops	11,995	341
HUC_1029	81	Hay/Pasture	23,935	297
HUC_1304	52	Shrub/Scrub	1,733	995
HUC_1601	52	Shrub/Scrub	2,642	1981
HUC_1708	42	Evergreen Forest	1,986	552
HUC_1711	42	Evergreen Forest	6,562	621
HUC_1805	52	Shrub/Scrub	1,208	222
HUC_1808	52	Shrub/Scrub	1,089	1625

824



825

826 **Figure B1.** Comparison of floodplain extents derived from GFPlain90 (this study) and GFPlain250 (Nardi et al.,
827 2019). The right-hand panels are the inset area outlined in the orange box on the left panels; the top panels represent
828 an eastern coastal watershed (HUC_0304) whereas the bottom panels are from a midwestern US watershed
829 (HUC_1024). The full extent of the riverine network is evident in the GFPlain90 dataset, which was derived from 90
830 m resolution DEMs in contrast to the 250 m pixel size of the GFPlain250. Satellite imagery sourced from ESRI
831 (2022).



832 **References**

833

834 Adame, M. F., Arthington, A. H., Waltham, N., Hasan, S., Selles, A., and Ronan, M.: Managing threats
835 and restoring wetlands within catchments of the Great Barrier Reef, Australia, *Aquatic Conservation:
836 Marine and Freshwater Ecosystems*, 29, 829-839, <https://doi.org/10.1002/aqc.3096>, 2019.

837 Alfieri, L., Salamon, P., Bianchi, A., Neal, J., Bates, P., and Feyen, L.: Advances in pan-European flood
838 hazard mapping, *Hydrological Processes*, 28, 4067-4077, 10.1002/hyp.9947, 2014.

839 Ameli, A. A. and Creed, I. F.: Does Wetland Location Matter When Managing Wetlands for Watershed-
840 Scale Flood and Drought Resilience?, *JAWRA Journal of the American Water Resources Association*,
841 55, 529-542, 10.1111/1752-1688.12737, 2019.

842 Aronica, G., Bates, P. D., and Horritt, M. S.: Assessing the uncertainty in distributed model predictions
843 using observed binary pattern information within GLUE, *Hydrological Processes*, 16, 2001-2016,
844 <https://doi.org/10.1002/hyp.398>, 2002.

845 Assessment, M. E.: *Ecosystems and Human Well-Being: Wetlands and Water Synthesis*, World
846 Resources Institute, Washington, D.C., 2005.

847 Badiou, P., Page, B., and Akinremi, W.: Phosphorus Retention in Intact and Drained Prairie Wetland
848 Basins: Implications for Nutrient Export, *Journal of Environmental Quality*, 47, 902-913,
849 <https://doi.org/10.2134/jeq2017.08.0336>, 2018.

850 Bam, E. K. P., Ireson, A. M., van der Kamp, G., and Hendry, J. M.: Ephemeral Ponds: Are They the
851 Dominant Source of Depression-Focused Groundwater Recharge?, *Water Resources Research*, 56,
852 e2019WR026640, <https://doi.org/10.1029/2019WR026640>, 2020.

853 Bates, P. D. and De Roo, A. P. J.: A simple raster-based model for flood inundation simulation, *Journal of*
854 *Hydrology*, 236, 54-77, [http://dx.doi.org/10.1016/S0022-1694\(00\)00278-X](http://dx.doi.org/10.1016/S0022-1694(00)00278-X), 2000.

855 Beck, H. E., Zimmermann, N. E., McVicar, T. R., Vergopolan, N., Berg, A., and Wood, E. F.: Present
856 and future Köppen-Geiger climate classification maps at 1-km resolution, *Scientific Data*, 5, 180214,
857 10.1038/sdata.2018.214, 2018.



- 858 Berhane, T., Lane, C., Wu, Q., Autrey, B., Anenkhnov, O., Chepinoga, V., and Liu, H.: Decision-Tree,
859 Rule-Based, and Random Forest Classification of High-Resolution Multispectral Imagery for Wetland
860 Mapping and Inventory, *Remote Sensing*, 10, 580, 2018.
- 861 Biggs, J., von Fumetti, S., and Kelly-Quinn, M.: The importance of small waterbodies for biodiversity
862 and ecosystem services: implications for policy makers, *Hydrobiologia*, 793, 3-39, 10.1007/s10750-
863 016-3007-0, 2017.
- 864 Blanchette, M., Rousseau, A. N., Savary, S., and Foulon, É.: Are spatial distribution and aggregation of
865 wetlands reliable indicators of stream flow mitigation?, *Journal of Hydrology*, 608, 127646,
866 <https://doi.org/10.1016/j.jhydrol.2022.127646>, 2022.
- 867 Brown, C. F., Brumby, S. P., Guzder-Williams, B., Birch, T., Hyde, S. B., Mazzariello, J., Czerwinski,
868 W., Pasquarella, V. J., Haertel, R., Ilyushchenko, S., Schwehr, K., Weisse, M., Stolle, F., Hanson, C.,
869 Guinan, O., Moore, R., and Tait, A. M.: Dynamic World, Near real-time global 10 m land use land
870 cover mapping, *Scientific Data*, 9, 251, 10.1038/s41597-022-01307-4, 2022.
- 871 Buttle, J. M.: Mediating stream baseflow response to climate change: The role of basin storage,
872 *Hydrological Processes*, 32, 363-378, 10.1002/hyp.11418, 2018.
- 873 Chen, J., Chen, J., Liao, A., Cao, X., Chen, L., Chen, X., He, C., Han, G., Peng, S., Lu, M., Zhang, W.,
874 Tong, X., and Mills, J.: Global land cover mapping at 30m resolution: A POK-based operational
875 approach, *ISPRS Journal of Photogrammetry and Remote Sensing*, 103, 7-27,
876 <https://doi.org/10.1016/j.isprsjprs.2014.09.002>, 2015.
- 877 Chen, W., Thorslund, J., Nover, D. M., Rains, M. C., Li, X., Xu, B., He, B., Su, H., Yen, H., Liu, L.,
878 Yuan, H., Jarsjö, J., and Viers, J. H.: A typological framework of non-floodplain wetlands for global
879 collaborative research and sustainable use, *Environmental Research Letters*, 17, 113002, 10.1088/1748-
880 9326/ac9850, 2022.
- 881 Cheng, F. Y. and Basu, N. B.: Biogeochemical hotspots: Role of small water bodies in landscape nutrient
882 processing, *Water Resources Research*, 53, 5038-5056, 10.1002/2016WR020102, 2017.



- 883 Cheng, F. Y., Van Meter, K. J., Byrnes, D. K., and Basu, N. B.: Maximizing US nitrate removal through
884 wetland protection and restoration, *Nature*, 588, 625-630, 10.1038/s41586-020-03042-5, 2020.
- 885 Christensen, J. R., Golden, H. E., Alexander, L. C., Pickard, B. R., Fritz, K. M., Lane, C. R., Weber, M.
886 H., Kwok, R. M., and Keefer, M. N.: Headwater streams and inland wetlands: Status and advancements
887 of geospatial datasets and maps across the United States, *Earth-Science Reviews*, 104230,
888 <https://doi.org/10.1016/j.earscirev.2022.104230>, 2022.
- 889 Cohen, M. J., Creed, I. F., Alexander, L., Basu, N. B., Calhoun, A. J. K., Craft, C., D'Amico, E.,
890 DeKeyser, E., Fowler, L., Golden, H. E., Jawitz, J. W., Kalla, P., Kirkman, L. K., Lane, C. R., Lang,
891 M., Leibowitz, S. G., Lewis, D. B., Marton, J., McLaughlin, D. L., Mushet, D. M., Raanan-Kiperwas,
892 H., Rains, M. C., Smith, L., and Walls, S. C.: Do geographically isolated wetlands influence landscape
893 functions?, *Proceedings of the National Academy of Sciences*, 113, 1978-1986,
894 10.1073/pnas.1512650113, 2016.
- 895 Colvin, S. A. R., Sullivan, S. M. P., Shirey, P. D., Colvin, R. W., Winemiller, K. O., Hughes, R. M.,
896 Fausch, K. D., Infante, D. M., Olden, J. D., Bestgen, K. R., Danehy, R. J., and Eby, L.: Headwater
897 Streams and Wetlands are Critical for Sustaining Fish, Fisheries, and Ecosystem Services, *Fisheries*, 44,
898 73-91, 2019.
- 899 Cowardin, L. M., Carter, V., Golet, F. C., and LaRoe, E. T.: Classification of Wetlands and Deepwater
900 habitats of The United States, Fish and Wildlife Service, Washington DCFWS/OBS-79/31, 1979.
- 901 Creed, I. F., Lane, C. R., Serran, J. N., Alexander, L. C., Basu, N. B., Calhoun, A. J. K., Christensen, J.
902 R., Cohen, M. J., Craft, C., D'Amico, E., DeKeyser, E., Fowler, L., Golden, H. E., Jawitz, J. W., Kalla,
903 P., Kirkman, L. K., Lang, M., Leibowitz, S. G., Lewis, D. B., Marton, J., McLaughlin, D. L., Raanan-
904 Kiperwas, H., Rains, M. C., Rains, K. C., and Smith, L.: Enhancing protection for vulnerable waters,
905 *Nature Geoscience*, 10, 809-815, 10.1038/ngeo3041, 2017.
- 906 Cunha, D. G. F., Magri, R. A. F., Tromboni, F., Ranieri, V. E. L., Fendrich, A. N., Campanhão, L. M. B.,
907 Riveros, E. V., and Velázquez, J. A.: Landscape patterns influence nutrient concentrations in aquatic



908 systems: citizen science data from Brazil and Mexico, *Freshwater Science*, 38, 365-378,
909 10.1086/703396, 2019.

910 Dahl, T. E.: Wetlands - Losses in the United States, 1780's to 1980's, U.S. Department of Interior, Fish
911 and Wildlife Service Washington DC, 1990.

912 Davidson, N. C.: How much wetland has the world lost? Long-term and recent trends in global wetland
913 area, *Marine and Freshwater Research*, 65, 934-941, <http://dx.doi.org/10.1071/MF14173>, 2014.

914 De Groot, R., M. Stuij, M. Finlayson, and N. Davidson: Valuing Wetlands: Guidance for Valuing the
915 Benefits Derived from Wetland Ecosystem Services, Ramsar Convention Secretariat, Gland,
916 Switzerland and Secretariat of the Convention on Biological Diversity, Montreal, Canada, Gland,
917 Switzerland Ramsar Technical Report No. 3/CBD Technical Series No. 27, 2006.

918 DeVries, B., Huang, C., Lang, M., Jones, J., Huang, W., Creed, I., and Carroll, M.: Automated
919 Quantification of Surface Water Inundation in Wetlands Using Optical Satellite Imagery, *Remote
920 Sensing*, 9, 807, 2017.

921 Dewitz, J.: National Land Cover Database (NLCD) 2016 Products: U.S. Geological Survey data release
922 [dataset], <https://doi.org/10.5066/P96HHBIE>, 2019.

923 Drenkhan, F., Buytaert, W., Mackay, J. D., Barrand, N. E., Hannah, D. M., and Huggel, C.: Looking
924 beyond glaciers to understand mountain water security, *Nature Sustainability*, 10.1038/s41893-022-
925 00996-4, 2022.

926 ESA Worldwide Land Cover Mapping: <https://esa-worldcover.org/en>, last access: 22 December 2022.
927 ESA Land Cover CCI, Product User Guide Version 2.0:
928 https://maps.elie.ucl.ac.be/CCI/viewer/download/ESACCI-LC-Ph2-PUGv2_2.0.pdf, last access: May
929 2022.

930 ESRI World Terrain Base
931 <https://www.arcgis.com/home/item.html?id=be2e229ffc864c868a78f5ca68ca5b8e>, last accessed 22
932 December 2022.



- 933 Evenson, G. R., Golden, H. E., Lane, C. R., McLaughlin, D. L., and D'Amico, E.: Depressional Wetlands
934 Affect Watershed Hydrological, Biogeochemical, and Ecological Functions, Ecological Applications,
935 28, 953-966, 10.1002/eap.1701, 2018a.
- 936 Evenson, G. R., Jones, C. N., McLaughlin, D. L., Golden, H. E., Lane, C. R., DeVries, B., Alexander, L.
937 C., Lang, M. W., McCarty, G. W., and Sharifi, A.: A watershed-scale model for depressional wetland-
938 rich landscapes, Journal of Hydrology X, 1, 100002, <https://doi.org/10.1016/j.hydroa.2018.10.002>,
939 2018b.
- 940 Evenson, G. R., Golden, H. E., Christensen, J. R., Lane, C. R., Rajib, A., D'Amico, E., Mahoney, D. T.,
941 White, E., and Wu, Q.: Wetland restoration yields dynamic nitrate responses across the Upper
942 Mississippi river basin, Environmental Research Communications, 3, 095002, 10.1088/2515-
943 7620/ac2125, 2021.
- 944 Fan, Y., Li, H., and Miguez-Macho, G.: Global Patterns of Groundwater Table Depth, Science, 339, 940-
945 943, doi:10.1126/science.1229881, 2013.
- 946 Fewtrell, T. J., Bates, P. D., Horritt, M., and Hunter, N. M.: Evaluating the effect of scale in flood
947 inundation modelling in urban environments, Hydrological Processes, 22, 5107-5118,
948 <https://doi.org/10.1002/hyp.7148>, 2008.
- 949 Fluet-Chouinard, E., Lehner, B., Rebelo, L.-M., Papa, F., and Hamilton, S. K.: Development of a global
950 inundation map at high spatial resolution from topographic downscaling of coarse-scale remote sensing
951 data, Remote Sensing of Environment, 158, 348-361, <https://doi.org/10.1016/j.rse.2014.10.015>, 2015.
- 952 Fossey, M. and Rousseau, A. N.: Can isolated and riparian wetlands mitigate the impact of climate
953 change on watershed hydrology? A case study approach, Journal of Environmental Management,
954 184(2):327-339, <http://dx.doi.org/10.1016/j.jenvman.2016.09.043>, 2016.
- 955 Golden, H. E., Lane, C. R., Rajib, A., and Wu, Q.: Improving global flood and drought predictions:
956 integrating non-floodplain wetlands into watershed hydrologic models, Environmental Research
957 Letters, 16, 091002, 10.1088/1748-9326/ac1fbc, 2021.



- 958 Golden, H. E., Rajib, A., Lane, C. R., Christensen, J. R., Wu, Q., and Mengistu, S.: Non-floodplain
959 Wetlands Affect Watershed Nutrient Dynamics: A Critical Review, *Environmental Science &*
960 *Technology*, 53, 7203-7214, 10.1021/acs.est.8b07270, 2019.
- 961 Golden, H. E., Sander, H. A., Lane, C. R., Zhao, C., Price, K., D'Amico, E., and Christensen, J. R.:
962 Relative effects of geographically isolated wetlands on streamflow: a watershed-scale analysis,
963 *Ecohydrology*, 9, 21-38, 10.1002/eco.1608, 2016.
- 964 Golden, H. E., Creed, I. F., Ali, G., Basu, N. B., Neff, B. P., Rains, M. C., McLaughlin, D. L., Alexander,
965 L. C., Ameli, A. A., Christensen, J. R., Evenson, G. R., Jones, C. N., Lane, C. R., and Lang, M.:
966 Integrating geographically isolated wetlands into land management decisions, *Frontiers in Ecology and*
967 *the Environment*, 15, 319-327, 10.1002/fee.1504, 2017.
- 968 Gumbrecht, T., Roman-Cuesta, R. M., Verchot, L., Herold, M., Wittmann, F., Householder, E., Herold,
969 N., and Murdiyarso, D.: An expert system model for mapping tropical wetlands and peatlands reveals
970 South America as the largest contributor, *Global Change Biology*, 23, 3581-3599,
971 <https://doi.org/10.1111/gcb.13689>, 2017.
- 972 Hamunyela, E., Hipondoka, M., Persendt, F., Sevelia Nghiyalwa, H., Thomas, C., and Matengu, K.:
973 Spatio-temporal characterization of surface water dynamics with Landsat in endorheic Cuvelai-Etoshia
974 Basin (1990–2021), *ISPRS Journal of Photogrammetry and Remote Sensing*, 191, 68-84,
975 <https://doi.org/10.1016/j.isprsjprs.2022.07.007>, 2022.
- 976 Homer, C., Dewitz, J., Jin, S., Xian, G., Costello, C., Danielson, P., Gass, L., Funk, M., Wickham, J.,
977 Stehman, S., Auch, R., and Riitters, K.: Conterminous United States land cover change patterns 2001–
978 2016 from the 2016 National Land Cover Database, *ISPRS Journal of Photogrammetry and Remote*
979 *Sensing*, 162, 184-199, <https://doi.org/10.1016/j.isprsjprs.2020.02.019>, 2020.
- 980 Horritt, M. S. and Bates, P. D.: Evaluation of 1D and 2D numerical models for predicting river flood
981 inundation, *Journal of Hydrology*, 268, 87-99, [http://dx.doi.org/10.1016/S0022-1694\(02\)00121-X](http://dx.doi.org/10.1016/S0022-1694(02)00121-X),
982 2002.



- 983 Hu, S., Niu, Z., and Chen, Y.: Global Wetland Datasets: a Review, *Wetlands*, 37, 807-817,
984 10.1007/s13157-017-0927-z, 2017a.
- 985 Hu, S., Niu, Z., Chen, Y., Li, L., and Zhang, H.: Global wetlands: Potential distribution, wetland loss, and
986 status, *Science of The Total Environment*, 586, 319-327,
987 <http://dx.doi.org/10.1016/j.scitotenv.2017.02.001>, 2017b.
- 988 Huang, W., DeVries, B., Huang, C., Lang, M., Jones, J., Creed, I., and Carroll, M.: Automated Extraction
989 of Surface Water Extent from Sentinel-1 Data, *Remote Sensing*, 10, 797, 2018.
- 990 IPCC: Intergovernmental Panel on Climate Change 2014: Impacts, adaptation, and vulnerability,
991 Cambridge University Press, Cambridge, U.K.2014.
- 992 Jafarzadegan, K., Merwade, V., and Saksena, S.: A geomorphic approach to 100-year floodplain mapping
993 for the Conterminous United States, *Journal of Hydrology*, 561, 43-58,
994 <https://doi.org/10.1016/j.jhydrol.2018.03.061>, 2018.
- 995 Jakubínský, J., Prokopová, M., Raška, P., Salvati, L., Bezak, N., Cudlín, O., Cudlín, P., Purkyt, J., Vezza,
996 P., Camporeale, C., Daněk, J., Pástor, M., and Lepsška, T.: Managing floodplains using nature-based
997 solutions to support multiple ecosystem functions and services, *WIREs Water*, 8, e1545,
998 <https://doi.org/10.1002/wat2.1545>, 2021.
- 999 Jin, S., Homer, C., Yang, L., Danielson, P., Dewitz, J., Li, C., Zhu, Z., Xian, G., and Howard, D.: Overall
1000 Methodology Design for the United States National Land Cover Database 2016 Products, *Remote
1001 Sensing*, 11, 2971, 2019.
- 1002 Jones, C. N., Evenson, G. R., McLaughlin, D. L., Vanderhoof, M. K., Lang, M. W., McCarty, G. W.,
1003 Golden, H. E., Lane, C. R., and Alexander, L. C.: Estimating restorable wetland water storage at
1004 landscape scales, *Hydrological Processes*, 32, 305-313, 10.1002/hyp.11405, 2018.
- 1005 Kam, S. P.: Valuing the role of living aquatic resources to rural livelihoods in multiple-use, seasonally-
1006 inundated wetlands in the Yellow River Basin of China, for improved governance, CGIAR Challenge
1007 Program on Water & Food, Colombo, Sri Lanka, <https://hdl.handle.net/10568/3859>, 2010.



- 1008 Khare, A., Rajib, A., Zheng, Q., Golden, H. E., Wu, Q., Lane, C. R., Christensen, J. R., Dahl, T. A.,
1009 Ryder, J. L., and McFall, B. C.: Global surface water estimates: Critical need for data consistency and
1010 integration, *Nature Water*, in review.
- 1011 Kremenetski, K. V., Velichko, A. A., Borisova, O. K., MacDonald, G. M., Smith, L. C., Frey, K. E., and
1012 Orlova, L. A.: Peatlands of the Western Siberian lowlands: current knowledge on zonation, carbon
1013 content and Late Quaternary history, *Quaternary Science Reviews*, 22, 703-723, 2003.
- 1014 Kundzewicz, Z. W., Hegger, D. L. T., Matczak, P., and Driessen, P. P. J.: Opinion: Flood-risk reduction:
1015 Structural measures and diverse strategies, *Proceedings of the National Academy of Sciences*, 115,
1016 12321-12325, 10.1073/pnas.1818227115, 2018.
- 1017 Lane, C. R. and D'Amico, E.: Identification of Putative Geographically Isolated Wetlands of the
1018 Conterminous United States, *JAWRA Journal of the American Water Resources Association*, 52, 705-
1019 722, 10.1111/1752-1688.12421, 2016.
- 1020 Lane, C. R., Leibowitz, S. G., Autrey, B. C., LeDuc, S. D., and Alexander, L. C.: Hydrological, Physical,
1021 and Chemical Functions and Connectivity of Non-Floodplain Wetlands to Downstream Waters: A
1022 Review, *JAWRA Journal of the American Water Resources Association*, 54, 346-371, 10.1111/1752-
1023 1688.12633, 2018.
- 1024 Lane, C. R., Creed, I. F., Golden, H. E., Leibowitz, S. G., Mushet, D. M., Rains, M. C., Wu, Q.,
1025 D'Amico, E., Alexander, L. C., Ali, G. A., Basu, N. B., Bennett, M. G., Christensen, J. R., Cohen, M.
1026 J., Covino, T. P., DeVries, B., Hill, R. A., Jencso, K., Lang, M. W., McLaughlin, D. L., Rosenberry, D.
1027 O., Rover, J., and Vanderhoof, M. K.: Vulnerable Waters are Essential to Watershed Resilience,
1028 *Ecosystems*, 10.1007/s10021-021-00737-2, 2022.
- 1029 Lane, C. R., E. D'Amico, J. R. Christensen, H. E. Golden, Q. Wu, and A. Rajib. Global non-floodplain
1030 wetlands [dataset], https://gaftp.epa.gov/EPADDataCommons/ORD/Global_NonFloodplain_Wetlands/
1031 and <https://doi.org/10.23719/1528331>, 2023.
- 1032 Lehner, B. and Doll, P.: Development and validation of a global database of lakes, reservoirs and
1033 wetlands, *Journal of Hydrology*, 296, 1-22, 2004.



- 1034 Lehner, B. and Grill, G.: Global river hydrography and network routing: baseline data and new
1035 approaches to study the world's large river systems, *Hydrological Processes*, 27, 2171-2186,
1036 <https://doi.org/10.1002/hyp.9740>, 2013.
- 1037 Leibowitz, S.: Geographically Isolated Wetlands: Why We Should Keep the Term, *Wetlands*, 35, 997-
1038 1003, 10.1007/s13157-015-0691-x, 2015.
- 1039 Leibowitz, S. G.: Isolated wetlands and their functions: an ecological perspective, *Wetlands*, 22, 517-531,
1040 2003.
- 1041 Leibowitz, S. G., Hill, R. A., Creed, I. F., Compton, J. E., Golden, H. E., Weber, M. H., Rains, M. C.,
1042 Jones, J., C. E., Lee, E. H., Christensen, J. R., Bellmore, R. A., and Lane, C. R.: Connections matter:
1043 National classification links wetlands and water quality, *Science*, In Review.
- 1044 Liu, D., Cao, C., Chen, W., Ni, X., Tian, R., and Xing, X.: Monitoring and predicting the degradation of a
1045 semi-arid wetland due to climate change and water abstraction in the Ordos Larus relictus National
1046 Nature Reserve, China, *Geomatics, Natural Hazards and Risk*, 8, 367-383,
1047 10.1080/19475705.2016.1220024, 2017.
- 1048 Makungu, E. and Hughes, D. A.: Understanding and modelling the effects of wetland on the hydrology
1049 and water resources of large African river basins, *Journal of Hydrology*, 603, 127039,
1050 <https://doi.org/10.1016/j.jhydrol.2021.127039>, 2021.
- 1051 Martinis, S., Groth, S., Wieland, M., Knopp, L., and Rättich, M.: Towards a global seasonal and
1052 permanent reference water product from Sentinel-1/2 data for improved flood mapping, *Remote
1053 Sensing of Environment*, 278, 113077, <https://doi.org/10.1016/j.rse.2022.113077>, 2022.
- 1054 Marton, J. M., Creed, I. F., Lewis, D., Lane, C. R., Basu, N., Cohen, M. J., and C., C.: Geographically
1055 isolated wetlands are important biogeochemical reactors on the landscape, *BioScience*, 65, 408-418,
1056 10.1093/biosci/biv009, 2015.
- 1057 McCauley, L. A., Anteau, M. J., van der Burg, M. P., and Wiltermuth, M. T.: Land use and wetland
1058 drainage affect water levels and dynamics of remaining wetlands, *Ecosphere*, 6, art92, 10.1890/ES14-
1059 00494.1, 2015.



- 1060 McKenna, O. P., Mushet, D. M., Rosenberry, D. O., and LaBaugh, J. W.: Evidence for a climate-induced
1061 ecohydrological state shift in wetland ecosystems of the southern Prairie Pothole Region, *Climatic*
1062 *Change*, 145, 273-287, 10.1007/s10584-017-2097-7, 2017.
- 1063 McLaughlin, D. L., Kaplan, D. A., and Cohen, M. J.: A significant nexus: Geographically isolated
1064 wetlands influence landscape hydrology, *Water Resources Research*, 50, 7153-7166,
1065 10.1002/2013WR015002, 2014.
- 1066 Merken, R., Deboelpaep, E., Teunen, J., Saura, S., and Koedam, N.: Wetland Suitability and Connectivity
1067 for Trans-Saharan Migratory Waterbirds, *PLOS ONE*, 10, e0135445, 10.1371/journal.pone.0135445,
1068 2015.
- 1069 Messenger, M. L., Lehner, B., Grill, G., Nedeva, I., and Schmitt, O.: Estimating the volume and age of
1070 water stored in global lakes using a geo-statistical approach, *Nature Communications*, 7, 13603,
1071 10.1038/ncomms13603, 2016.
- 1072 Mushet, D., Calhoun, A., Alexander, L., Cohen, M., DeKeyser, E., Fowler, L., Lane, C., Lang, M., Rains,
1073 M., and Walls, S.: Geographically Isolated Wetlands: Rethinking a Misnomer, *Wetlands*, 35, 423-431,
1074 10.1007/s13157-015-0631-9, 2015.
- 1075 Mushet, D. M., Alexander, L. C., Bennett, M., Schofield, K., Christensen, J. R., Ali, G., Pollard, A., Fritz,
1076 K., and Lang, M. W.: Differing Modes of Biotic Connectivity within Freshwater Ecosystem Mosaics,
1077 *JAWRA Journal of the American Water Resources Association*, 55, 307-317, 10.1111/1752-
1078 1688.12683, 2019.
- 1079 Nardi, F., Annis, A., Di Baldassarre, G., Vivoni, E. R., and Grimaldi, S.: GFPLAIN250m, a global high-
1080 resolution dataset of Earth's floodplains, *Scientific Data*, 6, 180309, 10.1038/sdata.2018.309, 2019.
- 1081 National Landcover Database (NLCD) 2019 NLCD Land Cover (CONUS), <https://www.mrlc.gov/data>,
1082 last accessed 22 December 2022.



- 1083 Nitzsche, K. N., Kalettka, T., Premke, K., Lischeid, G., Gessler, A., and Kayler, Z. E.: Land-use and
1084 hydroperiod affect kettle hole sediment carbon and nitrogen biogeochemistry, *Science of The Total*
1085 *Environment*, 574, 46-56, <http://dx.doi.org/10.1016/j.scitotenv.2016.09.003>, 2017.
- 1086 Olefeldt, D., Hovemyr, M., Kuhn, M. A., Bastviken, D., Bohn, T. J., Connolly, J., Crill, P., Euskirchen, E.
1087 S., Finkelstein, S. A., Genet, H., Grosse, G., Harris, L. I., Heffernan, L., Helbig, M., Hugelius, G.,
1088 Hutchins, R., Juutinen, S., Lara, M. J., Malhotra, A., Manies, K., McGuire, A. D., Natali, S. M.,
1089 O'Donnell, J. A., Parmentier, F. J. W., Räsänen, A., Schädel, C., Sonnentag, O., Strack, M., Tank, S. E.,
1090 Treat, C., Varner, R. K., Virtanen, T., Warren, R. K., and Watts, J. D.: The Boreal–Arctic Wetland and
1091 Lake Dataset (BAWLD), *Earth Syst. Sci. Data*, 13, 5127-5149, 10.5194/essd-13-5127-2021, 2021.
- 1092 Pekel, J.-F., Cottam, A., Gorelick, N., and Belward, A. S.: High-resolution mapping of global surface
1093 water and its long-term changes, *Nature*, 540, 418-422, 10.1038/nature20584, 2016.
- 1094 Prigent, C., Papa, F., Aires, F., Rossow, W. B., and Matthews, E.: Global inundation dynamics inferred
1095 from multiple satellite observations, 1993–2000, *Journal of Geophysical Research: Atmospheres*, 112,
1096 <https://doi.org/10.1029/2006JD007847>, 2007.
- 1097 PRISM Climate Group, Parameter-elevation Regressions on Independent Slopes Model,
1098 prism.oregonstate.edu/, last accessed 22 December 2022.
- 1099 Rains, M. C., Leibowitz, S. G., Cohen, M. J., Creed, I. F., Golden, H. E., Jawitz, J. W., Kalla, P., Lane, C.
1100 R., Lang, M. W., and McLaughlin, D. L.: Geographically isolated wetlands are part of the hydrological
1101 landscape, *Hydrological Processes*, 30, 153-160, 10.1002/hyp.10610, 2016.
- 1102 Rajib, A., Golden, H. E., Lane, C. R., and Wu, Q.: Surface depression and wetland water storage
1103 improves major river basin hydrologic predictions, *Water Resources Research*, 56, e2019WR026561,
1104 <https://doi.org/10.1029/2019WR026561>, 2020.
- 1105 Rajib, A., Zheng, Q., Lane, C. R., Golden, H. E., Christensen, J. R., Isibor, I., and Johnson, K.: Human
1106 alterations of the world's floodplains *Scientific Data*, in review.



- 1107 Rajib, A., Zheng, Q., Golden, H. E., Wu, Q., Lane, C. R., Christensen, J. R., Morrison, R. R., Annis, A.,
1108 and Nardi, F.: The changing face of floodplains in the Mississippi River Basin detected by a 60-year
1109 land use change dataset, *Scientific Data*, 8, 271, 10.1038/s41597-021-01048-w, 2021.
- 1110 Robarts, R., Zhulidov, A., and Pavlov, D.: The State of knowledge about wetlands and their future under
1111 aspects of global climate change: the situation in Russia, *Aquatic Sciences*, 75, 27-38, 10.1007/s00027-
1112 011-0230-7, 2013.
- 1113 Rodrigues, L. N., Sano, E. E., Steenhuis, T. S., and Passo, D. P.: Estimation of Small Reservoir Storage
1114 Capacities with Remote Sensing in the Brazilian Savannah Region, *Water Resources Management*, 26,
1115 873-882, 10.1007/s11269-011-9941-8, 2012.
- 1116 Rodríguez-Rodríguez, M., Aguilera, H., Guardiola-Albert, C., and Fernández-Ayuso, A.: Climate
1117 Influence Vs. Local Drivers in Surface Water-Groundwater Interactions in Eight Ponds of Doñana
1118 National Park (Southern Spain), *Wetlands*, 41, 25, 10.1007/s13157-021-01425-6, 2021.
- 1119 Sampson, C. C., Smith, A. M., Bates, P. D., Neal, J. C., Alfieri, L., and Freer, J. E.: A high-resolution
1120 global flood hazard model, *Water Resources Research*, 51, 7358-7381, 10.1002/2015WR016954, 2015.
- 1121 Samways, M. J., Deacon, C., Kietzka, G. J., Pryke, J. S., Vorster, C., and Simaika, J. P.: Value of
1122 artificial ponds for aquatic insects in drought-prone southern Africa: a review, *Biodiversity and
1123 Conservation*, 29, 3131-3150, 10.1007/s10531-020-02020-7, 2020.
- 1124 Sangwan, N. and Merwade, V.: A Faster and Economical Approach to Floodplain Mapping Using Soil
1125 Information, *JAWRA Journal of the American Water Resources Association*, 51, 1286-1304,
1126 10.1111/1752-1688.12306, 2015.
- 1127 Schofield, K. A., Alexander, L. C., Ridley, C. E., Vanderhoof, M. K., Fritz, K. M., Autrey, B. C.,
1128 DeMeester, J. E., Kepner, W. G., Lane, C. R., Leibowitz, S. G., and Pollard, A. I.: Biota Connect
1129 Aquatic Habitats throughout Freshwater Ecosystem Mosaics, *JAWRA Journal of the American Water
1130 Resources Association*, 54, 372-399, 10.1111/1752-1688.12634, 2018.
- 1131 Serran, J. N., Creed, I. F., Ameli, A. A., and Aldred, D. A.: Estimating rates of wetland loss using power-
1132 law functions, *Wetlands*, 38, 109-120, 10.1007/s13157-017-0960-y, 2017.



- 1133 Shaw, D. A., Vanderkamp, G., Conly, F. M., Pietroniro, A., and Martz, L.: The Fill–Spill Hydrology of
1134 Prairie Wetland Complexes during Drought and Deluge, *Hydrological Processes*, 26, 3147-3156,
1135 10.1002/hyp.8390, 2012.
- 1136 Smith, L. L., Subalusky, A. L., Atkinson, C. L., Earl, J. E., Mushet, D. M., Scott, D. E., Lance, S. L., and
1137 Johnson, S. A.: Biological Connectivity of Seasonally Ponded Wetlands across Spatial and Temporal
1138 Scales, *JAWRA Journal of the American Water Resources Association*, 55, 334-353, 10.1111/1752-
1139 1688.12682, 2019.
- 1140 Strahler, A. N.: Quantitative analysis of watershed geomorphology, *American Geophysical Union*
1141 *Transactions*, 38, 913-920, 1957.
- 1142 Sullivan, S. M. P., Rains, M. C., and Rodewald, A. D.: Opinion: The proposed change to the definition of
1143 “waters of the United States” flouts sound science, *Proceedings of the National Academy of Sciences*,
1144 116, 11558, 10.1073/pnas.1907489116, 2019.
- 1145 Tayefi, V., Lane, S. N., Hardy, R. J., and Yu, D.: A comparison of one- and two-dimensional approaches
1146 to modelling flood inundation over complex upland floodplains, *Hydrological Processes*, 21, 3190-
1147 3202, 10.1002/hyp.6523, 2007.
- 1148 Tootchi, A., Jost, A., and Ducharne, A.: Multi-source global wetland maps combining surface water
1149 imagery and groundwater constraints, *Earth Syst. Sci. Data*, 11, 189-220, 10.5194/essd-11-189-2019,
1150 2019.
- 1151 Tsendbazar, N., Herold, M., Li, L., Tarko, A., de Bruin, S., Masiliunas, D., Lesiv, M., Fritz, S., Buchhorn,
1152 M., Smets, B., Van De Kerchove, R., and Duerauer, M.: Towards operational validation of annual
1153 global land cover maps, *Remote Sensing of Environment*, 266, 112686,
1154 <https://doi.org/10.1016/j.rse.2021.112686>, 2021.
- 1155 Tullos, D.: Opinion: How to achieve better flood-risk governance in the United States, *Proceedings of the*
1156 *National Academy of Sciences*, 115, 3731-3734, 10.1073/pnas.1722412115, 2018.



- 1157 Uden, D. R., Allen, C. R., Bishop, A. A., Grosse, R., Jorgensen, C. F., LaGrange, T. G., Stutheit, R. G.,
1158 and Vrtiska, M. P.: Predictions of future ephemeral springtime waterbird stopover habitat availability
1159 under global change, *Ecosphere*, 6, 1-26, 10.1890/ES15-00256.1, 2015.
- 1160 United States Geological Survey (USGS) National Elevation Dataset, <https://www.usgs.gov/3d-elevation->
1161 program, last accessed 22 December 2022.
- 1162 United States Geological Survey (USGS) Watershed Boundary Dataset, <https://www.usgs.gov/national->
1163 hydrography/access-national-hydrography-products, last accessed 22 December 2022.
- 1164 Van Meter, K. J. and Basu, N. B.: Signatures of human impact: size distributions and spatial organization
1165 of wetlands in the Prairie Pothole landscape, *Ecological Applications*, 25, 451-465, 10.1890/14-0662.1,
1166 2015.
- 1167 Van Meter, K. J., Basu, N. B., Tate, E., and Wyckoff, J.: Monsoon Harvests: The Living Legacies of
1168 Rainwater Harvesting Systems in South India, *Environmental Science & Technology*, 48, 4217-4225,
1169 10.1021/es4040182, 2014.
- 1170 Vanderhoof, M. K. and Lane, C. R.: The potential role of very high-resolution imagery to characterise
1171 lake, wetland and stream systems across the Prairie Pothole Region, United States, *International Journal*
1172 *of Remote Sensing*, 40, 5768-5798, 10.1080/01431161.2019.1582112, 2019.
- 1173 Wania, R., Melton, J. R., Hodson, E. L., Poulter, B., Ringeval, B., Spahni, R., Bohn, T., Avis, C. A.,
1174 Chen, G., Eliseev, A. V., Hopcroft, P. O., Riley, W. J., Subin, Z. M., Tian, H., van Bodegom, P. M.,
1175 Kleinen, T., Yu, Z. C., Singarayer, J. S., Zürcher, S., Lettenmaier, D. P., Beerling, D. J., Denisov, S. N.,
1176 Prigent, C., Papa, F., and Kaplan, J. O.: Present state of global wetland extent and wetland methane
1177 modelling: methodology of a model inter-comparison project (WETCHIMP), *Geosci. Model Dev.*, 6,
1178 617-641, 10.5194/gmd-6-617-2013, 2013.
- 1179 Werner, M. G. F., Hunter, N. M., and Bates, P. D.: Identifiability of distributed floodplain roughness
1180 values in flood extent estimation, *Journal of Hydrology*, 314, 139-157,
1181 <https://doi.org/10.1016/j.jhydrol.2005.03.012>, 2005.



- 1182 Wickham, J., Stehman, S. V., Sorenson, D. G., Gass, L., and Dewitz, J. A.: Thematic accuracy assessment
1183 of the NLCD 2016 land cover for the conterminous United States, *Remote Sensing of Environment*,
1184 257, 112357, <https://doi.org/10.1016/j.rse.2021.112357>, 2021.
- 1185 Wing, O. E. J., Bates, P. D., Sampson, C. C., Smith, A. M., Johnson, K. A., and Erickson, T. A.:
1186 Validation of a 30 m resolution flood hazard model of the conterminous United States, *Water Resources*
1187 *Research*, 53, 7968-7986, 10.1002/2017WR020917, 2017.
- 1188 Winter, T. C.: The Vulnerability of Wetlands to Climate Change: A Hydrologic Landscape Perspective,
1189 *JAWRA Journal of the American Water Resources Association*, 36, 305-311, 10.1111/j.1752-
1190 1688.2000.tb04269.x, 2000.
- 1191 Winter, T. C., J.W. Harvey, O.L. Franke, and Alley, W. M.: *Ground Water and Surface Water: A Single*
1192 *Resoure*, U.S. Government Printing Office, Washington, DC., 1998.
- 1193 Woznicki, S. A., Baynes, J., Panlasigui, S., Mehaffey, M., and Neale, A.: Development of a spatially
1194 complete floodplain map of the conterminous United States using random forest, *Science of The Total*
1195 *Environment*, 647, 942-953, <https://doi.org/10.1016/j.scitotenv.2018.07.353>, 2019.
- 1196 Wu, Q., Lane, C. R., Wang, L., Vanderhoof, M. K., Christensen, J. R., and Liu, H.: Efficient Delineation
1197 of Nested Depression Hierarchy in Digital Elevation Models for Hydrological Analysis Using Level-Set
1198 Method, *JAWRA Journal of the American Water Resources Association*, 55, 354-368, 10.1111/1752-
1199 1688.12689, 2019a.
- 1200 Wu, Q., Lane, C. R., Li, X., Zhao, K., Zhou, Y., Clinton, N., DeVries, B., Golden, H. E., and Lang, M.
1201 W.: Integrating LiDAR data and multi-temporal aerial imagery to map wetland inundation dynamics
1202 using Google Earth Engine, *Remote Sensing of Environment*, 228, 1-13,
1203 <https://doi.org/10.1016/j.rse.2019.04.015>, 2019b.
- 1204 Xi, Y., Peng, S., Ducharne, A., Ciais, P., Gumbrecht, T., Jimenez, C., Poulter, B., Prigent, C., Qiu, C.,
1205 Saunois, M., and Zhang, Z.: Gridded maps of wetlands dynamics over mid-low latitudes for 1980–2020
1206 based on TOPMODEL, *Scientific Data*, 9, 347, 10.1038/s41597-022-01460-w, 2022.



1207 Yamazaki, D., Ikeshima, D., Sosa, J., Bates, P. D., Allen, G., and Pavelsky, T.: MERIT Hydro: A high-
1208 resolution global hydrography map based on latest topography datasets, *Water Resources Research*, 55,
1209 5053-5073, 10.1029/2019wr024873, 2019.

1210 Zanaga, D., Van De Kerchove, R., De Keersmaecker, W., Souverijns, N., Brockmann, C., Quast, R.,
1211 Wevers, J., Grosu, A., Paccini, A., Vergnaud, S., Cartus, O., Santoro, M., Fritz, S., Georgieva, I., Lesiv,
1212 M., Carter, S., Herold, M., Li, Linlin, Tsendbazar, N.E., Ramoino, F., Arino, O.: ESA WorldCover 10
1213 m 2020 v100, <https://doi.org/10.5281/zenodo.5571936> 2021.

1214 Zedler, J. B. and Kercher, S.: Causes and consequences of invasive plants in wetlands: Opportunities,
1215 opportunists, and outcomes, *Critical Reviews in Plant Sciences*, 23, 431-452, 2004.

1216 Zhu, Y., Xu, Y., Deng, X., Kwon, H., and Qin, Z.: Peatland Loss in Southeast Asia Contributing to U.S.
1217 Biofuel's Greenhouse Gas Emissions, *Environmental Science & Technology*, 10.1021/acs.est.2c01561,
1218 2022.

1219